We are IntechOpen,
the world's leading publisher of
Open Access books
Built by scientists, for scientists

4,800

Open access books available

122,000

International authors and editors

135M

Downloads

Our authors are among the

154

Countries delivered to

TOP 1%

most cited scientists

12.2%

Contributors from top 500 universities

WEB OF SCIENCE™

Selection of our books indexed in the Book Citation Index
in Web of Science™ Core Collection (BKCI)

Interested in publishing with us?
Contact book.department@intechopen.com

Numbers displayed above are based on latest data collected.
For more information visit www.intechopen.com

Neural Network Control and Wireless Sensor Network-based Localization of Quadrotor UAV Formations

Travis Dierks and S. Jagannathan
Missouri University of Science and Technology
United States of America

1. Introduction

In recent years, quadrotor helicopters have become a popular unmanned aerial vehicle (UAV) platform, and their control has been undertaken by many researchers (Dierks & Jagannathan, 2008). However, a team of UAV's working together is often more effective than a single UAV in scenarios like surveillance, search and rescue, and perimeter security. Therefore, the formation control of UAV's has been proposed in the literature.

Saffarian and Fahimi present a modified leader-follower framework and propose a model predictive nonlinear control algorithm to achieve the formation (Saffarian & Fahimi, 2008). Although the approach is verified via numerical simulations, proof of convergence and stability is not provided. In the work of Fierro et al., cylindrical coordinates and contributions from wheeled mobile robot formation control (Desai et al., 1998) are considered in the development of a leader-follower based formation control scheme for aircrafts whereas the complete dynamics are assumed to be known (Fierro et al., 2001). The work by Gu et al. proposes a solution to the leader-follower formation control problem involving a linear inner loop and nonlinear outer-loop control structure, and experimental results are provided (Gu et al., 2006). The associated drawbacks are the need for a dynamic model and the measured position and velocity of the leader has to be communicated to its followers. Xie et al. present two nonlinear robust formation controllers for UAV's where the UAV's are assumed to be flying at a constant altitude. The first approach assumes that the velocities and accelerations of the leader UAV are known while the second approach relaxes this assumption (Xie et al., 2005). In both the designs, the dynamics of the UAV's are assumed to be available. Then, Galzi and Shtessel propose a robust formation controller based on higher order sliding mode controllers in the presence of bounded disturbances (Galzi & Shtessel, 2006).

In this work, we propose a new leader-follower formation control framework for quadrotor UAV's based on spherical coordinates where the desired position of a follower UAV is specified using a desired separation, s_d, and a desired- angle of incidence, α_d and bearing, β_d. Then, a new control law for leader-follower formation control is derived using neural networks (NN) to learn the complete dynamics of the UAV online, including unmodeled dynamics like aerodynamic friction in the presence of bounded disturbances. Although a

quadrotor UAV is underactuated, a novel NN virtual control input scheme for leader follower formation control is proposed which allows all six degrees of freedom of the UAV to be controlled using only four control inputs. Finally, we extend a graph theory-based scheme for discovery, localization and cooperative control. Discovery allows the UAV's to form into an ad hoc mobile sensor network whereas localization allows each UAV to estimate its position and orientation relative to its neighbors and hence the formation shape. This chapter is organized as follows. First, in Section 2, the leader-follower formation control problem for UAV's is introduced, and required background information is presented. Then, the NN control law is developed for the follower UAV's as well as the formation leader, and the stability of the overall formation is presented in Section 3. In Section 4, the localization and routing scheme is introduced for UAV formation control while Section 5 presents numerical simulations, and Section 6 provides some concluding remarks.

2. Background

2.1 Quadrotor UAV Dynamics

Consider a quadrotor UAV with six DOF defined in the inertial coordinate frame , E^a , as $[x, y, z, \phi, \theta, \psi]^T \in E^a$ where $\rho = [x, y, z]^T \in E^a$ are the position coordinates of the UAV and $\Theta = [\phi, \theta, \psi]^T \in E^a$ describe its orientation referred to as roll, pitch, and yaw, respectively. The translational and angular velocities are expressed in the body fixed frame attached to the center of mass of the UAV, E^b , and the dynamics of the UAV in the body fixed frame can be written as (Dierks & Jagannathan, 2008)

$$M \begin{bmatrix} \dot{v} \\ \dot{\omega} \end{bmatrix} = \bar{S}(\omega) \begin{bmatrix} v \\ \omega \end{bmatrix} + \begin{bmatrix} N_1(v) \\ N_2(\omega) \end{bmatrix} + \begin{bmatrix} G(R) \\ 0_{3x1} \end{bmatrix} + U + \tau_d \tag{1}$$

where $U = \begin{bmatrix} 0 & 0 & u_1 & u_2^T \end{bmatrix}^T \in \Re^6$,

$$M = \begin{bmatrix} mI_{3x3} & 0_{3x3} \\ 0_{3x3} & J \end{bmatrix} \in \Re^{6x6}, \quad \bar{S}(\omega) = \begin{bmatrix} -mS(\omega) & 0_{3x3} \\ 0_{3x3} & S(J\omega) \end{bmatrix} \in \Re^{6x6}$$

and m is a positive scalar that represents the total mass of the UAV, $J \in \Re^{3x3}$ represents the positive definite inertia matrix, $v(t) = [v_{xb}, v_{yb}, v_{zb}]^T \in \Re^3$ represents the translational velocity, $\omega(t) = [\omega_{xb}, \omega_{yb}, \omega_{zb}]^T \in \Re^3$ represents the angular velocity, $N_i(\bullet) \in \Re^{3x1}, i = 1, 2$, are the nonlinear aerodynamic effects, $u_1 \in \Re^1$ provides the thrust along the z-direction, $u_2 \in \Re^3$ provides the rotational torques, $\tau_d = [\tau_{d1}^T, \tau_{d2}^T]^T \in \Re^6$ and $\tau_{di} \in \Re^3$, $i = 1, 2$ represents unknown, but bounded disturbances such that $\|\tau_d\| < \tau_M$ for all time t , with τ_M being a known positive constant, $I_{nxn} \in \Re^{nxn}$ is an nxn identity matrix, and $0_{mxl} \in \Re^{mxl}$ represents an mxl matrix of all zeros. Furthermore, $G(R) \in \Re^3$ represents the

gravity vector defined as $G(R) = mgR^T(\Theta)E_z$ where $E_z = [0,0,1]^T$ is a unit vector in the inertial coordinate frame, $g = 9.81 m/s^2$, and $S(\bullet) \in \Re^{3x3}$ is the general form of a skew symmetric matrix defined as in (Dierks & Jagannathan, 2008). It is important to highlight $w^T S(\gamma)w = 0$ for any vector $w \in \Re^3$, and this property is commonly referred to as the *skew symmetric property* (Lewis et al., 1999).

The matrix $R(\Theta) \in \Re^{3x3}$ is the translational rotation matrix which is used to relate a vector in the body fixed frame to the inertial coordinate frame defined as (Dierks & Jagannathan, 2008)

$$R(\Theta) = R = \begin{bmatrix} c_\theta c_\psi & s_\phi s_\theta c_\psi - c_\phi s_\psi & c_\phi s_\theta c_\psi + s_\phi s_\psi \\ c_\theta s_\psi & s_\phi s_\theta s_\psi + c_\phi c_\psi & c_\phi s_\theta s_\psi - s_\phi c_\psi \\ -s_\theta & s_\phi c_\theta & c_\phi c_\theta \end{bmatrix} \tag{2}$$

where the abbreviations $s_{(\bullet)}$ and $c_{(\bullet)}$ have been used for $\sin(\bullet)$ and $\cos(\bullet)$, respectively. It is important to note that $R^{-1} = R^T$, $\dot{R} = RS(\omega)$ and $\dot{R}^T = -S(\omega)R^T$. It is also necessary to define a rotational transformation matrix from the fixed body to the inertial coordinate frame as (Dierks & Jagannathan, 2008)

$$T(\Theta) = T = \begin{bmatrix} 1 & s_\phi t_\theta & c_\phi t_\theta \\ 0 & c_\phi & -s_\phi \\ 0 & s_\phi/c_\theta & c_\phi/c_\theta \end{bmatrix} \tag{3}$$

where the abbreviation $t_{(\bullet)}$ has been used for $\tan(\bullet)$. The transformation matrices R and T are nonsingular as long as $-(\pi/2) < \phi < (\pi/2)$, $-(\pi/2) < \theta < (\pi/2)$ and $-\pi \le \psi \le \pi$. These regions will be assumed throughout the development of this work, and will be referred to as the *stable operation regions* of the UAV. Under these flight conditions, it is observed that $\|R\|_F = R_{\max}$ and $\|T\|_F < T_{\max}$ for known constants $R_{\max}$ and $T_{\max}$ (Neff et al., 2007).

Finally, the kinematics of the UAV can be written as

$$\begin{aligned} \dot{\rho} &= Rv \\ \dot{\Theta} &= T\omega \end{aligned} \tag{4}$$

2.2 Neural Networks

In this work, two-layer NN's are considered consisting of one layer of randomly assigned constant weights $V_N \in \Re^{axL}$ in the first layer and one layer of tunable weights $W_N \in \Re^{Lxb}$ in the second with a inputs, b outputs, and L hidden neurons. A compromise is made here between tuning the number of layered weights with computational complexity. The *universal approximation property* for NN's (Lewis et al., 1999) states that for any smooth function $f_N(x_N)$, there exists a NN such that $f_N(x_N) = W_N^T \sigma(V_N^T x_N) + \varepsilon_N$ where ε_N is the bounded NN functional approximation error such that $\|\varepsilon_N\| < \varepsilon_M$, for a known constant ε_M

and $\sigma(\cdot):\Re^a \to \Re^L$ is the activation function in the hidden layers. It has been shown that by randomly selecting the input layer weights V_N, the activation function $\sigma(\bar{x}_N) = \sigma(V_N^T x_N)$ forms a stochastic basis, and thus the approximation property holds for all inputs, $x_N \in \Re^a$, in the compact set S. The sigmoid activation function is considered here. Furthermore, on any compact subset of $\Re^n$, the target NN weights are bounded by a known positive value, W_M, such that $\|W_N\|_F \le W_M$. For complete details of the NN and its properties, see (Lewis et al., 1999).

2.3 Three Dimensional Leader-Follower Formation Control

Throughout the development, the follower UAV's will be denoted with a subscript '*j*' while the formation leader will be denoted by the subscript '*i*'. To begin the development, an alternate reference frame is defined by rotating the inertial coordinate frame about the z-axis by the yaw angle of follower j, ψ_j, and denoted by E_j^a. In order to relate a vector in E^a to E_j^a, the transformation matrix is given by

$$R_{aj} = \begin{bmatrix} \cos\psi_j & \sin\psi_j & 0 \\ -\sin\psi_j & \cos\psi_j & 0 \\ 0 & 0 & 1 \end{bmatrix}, \tag{5}$$

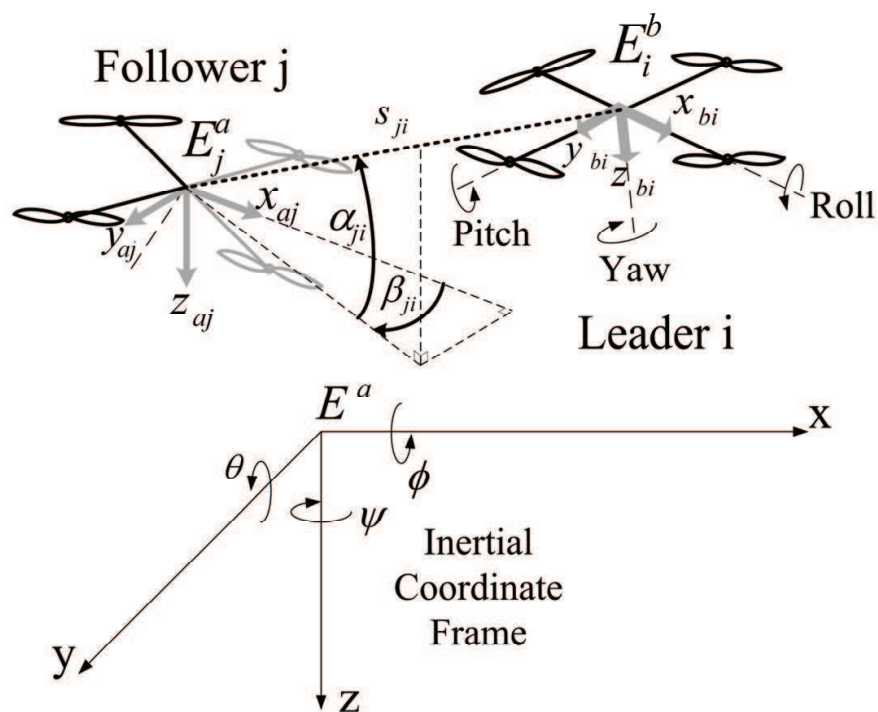where $R_{aj}^T = R_{aj}^{-1}$.

Figure 1. UAV leader-follower formation control

The objective of the proposed leader-follower formation control approach is for the follower UAV to maintain a desired separation, s_{jid}, at a desired angle of incidence, $\alpha_{jid} \in E_j^a$, and bearing, $\beta_{jid} \in E_j^a$, with respect to its leader. The incidence angle is measured from the $x_{aj}-y_{aj}$ plane of follower j while the bearing angle is measured from the positive x_{aj}-axis as shown in Figure 1. It is important to observe that each quantity is defined relative to the follower j instead of the leader i (Fierro et al., 2001), (Desai et al., 1998). Additionally, in order to specify a unique configuration of follower j with respect to its leader, the desired yaw of follower j is selected to be the yaw angle of leader i, $\psi_i \in E^a$ as in (Saffarian & Fahimi, 2008). Using this approach, the measured separation between follower j and leader i is written as

$$\rho_i - \rho_j = R_{aj}^T s_{ji} \Xi_{ji},$$ (6)

where

$$\Xi_{ji} = \begin{bmatrix} \cos\alpha_{ji}\cos\beta_{ji} \\ \cos\alpha_{ji}\sin\beta_{ji} \\ \sin\alpha_{ji} \end{bmatrix}.$$ (7)

Thus, to solve the leader-follower formation control problem in the proposed framework, a control velocity must be derived to ensure

$$\left. \begin{array}{l} \lim\limits_{t\to\infty}(s_{jid} - s_{ji}) = 0, \ \lim\limits_{t\to\infty}(\beta_{jid} - \beta_{ji}) = 0, \\ \lim\limits_{t\to\infty}(\alpha_{jid} - \alpha_{ji}) = 0, \ \lim\limits_{t\to\infty}(\psi_{jd} - \psi_j) = 0 \end{array} \right\}.$$ (8)

Throughout the development, s_{jid}, α_{jid} and β_{jid} will be taken as constants, while the constant total mass, m_j, is assumed to be known. Additionally, it will be assumed that reliable communication between the leader and its followers is available, and the leader communicates its measured orientation, Θ_i, and its *desired* states, $\psi_{id}, \dot\psi_{id}, \ddot\psi_{id}, v_{id}, \dot v_{id}$. This is a far less stringent assumption than assuming the leader communicates all of its *measured* states to its followers (Gu et al., 2006). Additionally, future work will relax this assumption. In the following section, contributions from single UAV control will be considered and extended to the leader-follower formation control of UAV's.

3. Leader-Follower Formation Tracking Control

In single UAV control literature, the overall control objective UAV j is often to track a desired trajectory, $\rho_{jd} = [x_{jd}, y_{jd}, z_{jd}]^T$, and a desired yaw ψ_{jd} while maintaining a stable flight configuration (Dierks & Jagannathan, 2008). The velocity v_{jzb} is directly

controllable with the thrust input. However, in order to control the translational velocities v_{jxb} and v_{jyb}, the pitch and roll must be controlled, respectively, thus redirecting the thrust. With these objectives in mind, the frameworks for single UAV control are extended to UAV formation control as follows.

3.1 Follower UAV Control Law

Given a leader i subject to the dynamics and kinematics (1) and (4), respectively, define a reference trajectory at a desired separation s_{jid}, at a desired angle of incidence, α_{jid}, and bearing, β_{jid} for follower j given by

$$\rho_{jd} = \rho_i - R_{ajd}^T s_{jid} \Xi_{jid} \tag{9}$$

where R_{ajd} is defined as in (5) and written in terms of ψ_{jd}, and Ξ_{jid} is written in terms of the desired angle of incidence and bearing, $\alpha_{jid}, \beta_{jid}$, respectively, similarly to (7). Next, using (6) and (9), define the position tracking error as

$$e_{j\rho} = \rho_{jd} - \rho_j = R_{aj}^T s_{ji} \Xi_{ji} - R_{ajd}^T s_{jid} \Xi_{jid} \in E^a \tag{10}$$

which can be measured using local sensor information. To form the position tracking error dynamics, it is convenient to rewrite (10) as $e_{j\rho} = \rho_i - \rho_j - R_{ajd}^T s_{jid} \Xi_{jid}$ revealing

$$\dot{e}_{j\rho} = R_i v_i - R_j v_j - \dot{R}_{ajd}^T s_{jid} \Xi_{jid}. \tag{11}$$

Next, select the desired translational velocity of follower j to stabilize (11)

$$v_{jd} = [v_{jdx} \ v_{jdy} \ v_{jdz}]^T = R_j^T \left(R_i v_{id} - \dot{R}_{ajd}^T s_{jid} \Xi_{jid} + K_{j\rho} e_{j\rho} \right) \in E^b \tag{12}$$

where $K_{j\rho} = diag\{k_{j\rho x}, k_{j\rho y}, k_{j\rho z}\} \in \Re^{3x3}$ is a diagonal positive definite design matrix of positive design constants and v_{id} is the desired translational velocity of leader i. Next, the translational velocity tracking error system is defined as

$$e_{jv} = \begin{bmatrix} e_{jvx} \\ e_{jvy} \\ e_{jvz} \end{bmatrix} = \begin{bmatrix} v_{jdx} \\ v_{jdy} \\ v_{jdz} \end{bmatrix} - \begin{bmatrix} v_{jxb} \\ v_{jyb} \\ v_{jzb} \end{bmatrix} = v_{jd} - v_j. \tag{13}$$

Applying (12) to (11) while observing $v_j = v_{jd} - e_{jv}$ and similarly $e_{iv} = v_{id} - v_i$, reveals the closed loop position error dynamics to be rewritten as

$$\dot{e}_{j\rho} = -K_{j\rho} e_{j\rho} + R_j e_{jv} - R_i e_{iv}. \tag{14}$$

Next, the translational velocity tracking error dynamics are developed. Differentiating (13), observing

$$\dot{v}_{jd} = -S(\omega_j)v_{jd} + R_j^T\left(R_iS(\omega_i)v_{id} + R_i\dot{v}_{id} - \ddot{R}_{ajd}^T s_{jid}\Xi_{jid}\right) + R_j^T K_{j\rho}\left(R_iv_i - R_jv_j - \dot{R}_{ajd}^T s_{jid}\Xi_{jid}\right),$$

substituting the translational velocity dynamics in (1), and adding and subtracting $R_j^T(K_{j\rho}(R_iv_{id} + R_jv_{jd}))$ reveals

$$\begin{aligned}\dot{e}_{jv} = \dot{v}_{jd} - \dot{v}_j &= -N_{j1}(v_j)/m_j - S(\omega_j)e_{jv} - G(R_j)/m_j - u_{j1}E_{jz}/m_j - \bar{\tau}_{jd1} \\ &+ R_j^T\left(R_iS(\omega_i)v_{id} + R_i\dot{v}_{id} - \ddot{R}_{ajd}s_{jid}\Xi_{jid} + K_{j\rho}\left(R_je_{jv} - K_{j\rho}e_{j\rho}\right)\right) - R_j^T K_{j\rho}(R_ie_{iv} - R_je_{jv})\end{aligned}$$ (15)

Next, we rewrite (2) in terms of the *scaled* desired orientation vector, $\bar{\Theta}_{jd} = [\bar{\theta}_{jd} \ \bar{\phi}_{jd} \ \psi_{jd}]^T$ where $\bar{\theta}_{jd} = \pi\theta_{jd}/(2\theta_{d\max})$, $\bar{\phi}_{jd} = \pi\phi_{jd}/(2\phi_{d\max})$, and $\theta_{d\max} \in (0, \pi/2)$ and $\phi_{d\max} \in (0, \pi/2)$ are the maximum desired roll and pitch, respectively, define $R_{jd} = R_j(\bar{\Theta}_{jd})$, and add and subtract $G(R_{jd})/m_j$ and $R_{jd}^T\Lambda_j$ with $\Lambda_j = R_i\dot{v}_{id} - \ddot{R}_{ajd}s_{jid}\Xi_{jid} + K_{j\rho}R_je_{jv} - K_{j\rho}e_{j\rho}$ to $\dot{e}_{jv}$ to yield

$$\dot{e}_{jv} = -G(R_{jd})/m_j + R_{jd}^T\Lambda_j + A_{jc1}f_{cj1}(x_{cj1}) - u_{j1}E_{jz}/m_j - K_{j\rho}R_ie_{iv} - \bar{\tau}_{jd1}$$ (16)

where $A_{jc1} = diag\{\cos(\bar{\theta}_{jd}), \cos(\bar{\phi}_{jd}), 1\} \in \Re^{3 \times 3}$ and

$$\begin{aligned}f_{cj1}(x_{cj1}) = A_{jc1}^{-1}\left(G(R_{jd})/m_j - G(R_j)/m_j + (R_j^T - R_{jd}^T)\Lambda_j\right) + \\ A_{jc1}^{-1}\left(K_{j\rho}R_je_{jv} - S(\omega_j)e_{jv} - N_{j1}(v_j)/m_j + R_j^T R_iS(\omega_i)v_{id} + R_j^T K_{j\rho}(1 - K_{j\rho})e_{j\rho}\right)\end{aligned}$$ (17)

is an unknown function which can be rewritten as $f_{jc1}(x_{jc1}) = \begin{bmatrix} f_{jc11} & f_{jc12} & f_{jc13} \end{bmatrix}^T \in \Re^3$. In the forthcoming development, the approximation properties of NN will be utilized to estimate the unknown function $f_{jc1}(x_{jc1})$ by bounded ideal weights W_{jc1}^T, V_{jc1}^T such that $\|W_{jc1}\|_F \le W_{Mc1}$ for an unknown constant W_{Mc1}, and written as $f_{jd}(x_{jd}) = W_{jd}^T\sigma(V_{jd}^T x_{jd}) + \varepsilon_{jd}$ where $\varepsilon_{jc1} \le \varepsilon_{Mc1}$ is the bounded NN approximation error where ε_{Mc1} is a known constant. The NN estimate of f_{jc1} is written as $\hat{f}_{jc1} = \hat{W}_{jc1}^T\sigma(V_{jc1}^T\hat{x}_{jc1}) = \hat{W}_{jc1}^T\hat{\sigma}_{jc1}$ $= [\hat{W}_{jc11}^T\hat{\sigma}_{jc1} \ \hat{W}_{jc12}^T\hat{\sigma}_{jc1} \ \hat{W}_{jc13}^T\hat{\sigma}_{jc1}]^T$ where $\hat{W}_{jc1}^T$ is the NN estimate of W_{jc1}^T, $\hat{W}_{jc1i}^T, i = 1,2,3$ is the ith row of $\hat{W}_{jc1}^T$, and $\hat{x}_{jc1}$ is the NN input defined as

$$\hat{x}_{jc1} = [1 \ \Theta_j^T \ \Theta_i^T \ \Lambda_j^T \ v_{jd}^T \ v_{id}^T \ \dot{v}_{id}^T \ \psi_{jd} \ \dot{\psi}_{jd} \ \ddot{\psi}_{jd} \ \omega_j^T \ v_j^T \ e_{jv}^T \ e_{j\rho}^T]^T.$$

Note that $\hat{x}_{jc1}$ is an estimate of x_{jc1} since the follower does not know ω_i. However, Θ_i is directly related to ω_i; therefore, it is included instead.

Remark 1: In the development of (16), the scaled desired orientation vector was utilized as a design tool to specify the desired pitch and roll angles. If the un-scaled desired orientation

vector was used instead, the maximum desired pitch and roll would remain within the stable operating regions. However, it is desirable to saturate the desired pitch and roll before they reach the boundaries of the stable operating region.

Next, the virtual control inputs θ_{jd} and ϕ_{jd} are identified to control the translational velocities v_{jxb} and v_{jyb}, respectively. The key step in the development is identifying the *desired* closed loop velocity tracking error dynamics. For convenience, the *desired* translational velocity closed loop system is selected as

$$\dot{e}_{jv} = -K_{jv}e_{jv} - \bar{\tau}_{jd1} - K_{j\rho}R_i e_{iv} \tag{18}$$

where $K_{jv} = diag\{k_{jv1}\cos(\bar{\theta}_{jd}), k_{jv2}\cos(\bar{\phi}_{jd}), k_{v3}\}$ is a diagonal positive definite design matrix with each $k_{vi} > 0$, $i = 1,2,3$, and $\bar{\tau}_{jd1} = \tau_{jd1}/m_j$. In the following development, it will be shown that $\theta_d \in (-\pi/2, \pi/2)$ and $\phi_d \in (-\pi/2, \pi/2)$; therefore, it is clear that $K_v > 0$. Then, equating (16) and (18) while considering only the first two velocity error states reveals

$$-g\begin{bmatrix} -s_{\bar{\theta}jd} \\ c_{\bar{\theta}jd}s_{\bar{\phi}jd} \end{bmatrix} + \begin{bmatrix} c_{\bar{\theta}jd}(k_{jv1}e_{jvx} + f_{jc11}) \\ c_{\bar{\phi}jd}(k_{jv2}e_{jvy} + f_{jc12}) \end{bmatrix} + \begin{bmatrix} c_{\bar{\theta}jd}c_{\psi jd} & c_{\bar{\theta}jd}s_{\psi jd} & -s_{\bar{\theta}jd} \\ s_{\bar{\phi}jd}s_{\bar{\theta}jd}c_{\psi jd} - c_{\bar{\phi}jd}s_{\psi jd} & s_{\bar{\phi}jd}s_{\bar{\theta}jd}s_{\psi jd} + c_{\bar{\phi}jd}c_{\psi jd} & s_{\bar{\phi}jd}c_{\bar{\theta}jd} \end{bmatrix}\begin{bmatrix} \Lambda_{j1} \\ \Lambda_{j2} \\ \Lambda_{j3} \end{bmatrix} = \begin{bmatrix} 0 \\ 0 \end{bmatrix} \tag{19}$$

where $\Lambda_j = [\Lambda_{j1} \ \Lambda_{j2} \ \Lambda_{j3}]^T$ was utilized. Then, applying basic math operations, the first line of (19) can be solved for the desired pitch θ_{jd} while the second line reveals the desired roll ϕ_{jd}. Using the NN estimates, $\hat{f}_{cj1}$, The desired pitch θ_{jd} can be written as

$$\theta_{jd} = \frac{2\theta_{\max}}{\pi} a\tan\left(\frac{N_{\theta jd}}{D_{\theta jd}}\right) \tag{20}$$

where $N_{\theta jd} = c_{\psi jd}\Lambda_{j1} + s_{\psi jd}\Lambda_{j2} + k_{jv1}e_{jvx} + \hat{f}_{jc11}$ and $D_{\theta jd} = \Lambda_{j3} - g$. Similarly, the desired roll angle, ϕ_{jd}, is found to be

$$\phi_{jd} = \frac{2\phi_{\max}}{\pi} a\tan\left(\frac{N_{\phi jd}}{D_{\phi jd}}\right) \tag{21}$$

where $N_{\phi jd} = s_{\psi jd}\Lambda_{j1} - c_{\psi jd}\Lambda_{j2} - k_{jv2}e_{jvy} + \hat{f}_{jc12}$ and $D_{\phi jd} = c_{\bar{\theta}jd}(\Lambda_{j3} - g) + s_{\bar{\theta}jd}c_{\psi jd}\Lambda_{j1} + s_{\bar{\theta}jd}s_{\psi jd}\Lambda_{j2}$.

Remark 2: The expressions for the desired pitch and roll in (20) and (21) lend themselves very well to the control of a quadrotor UAV. The expressions will always produce desired values in the *stable operation regions* of the UAV. It is observed that $a\tan(\bullet)$ approaches $\pm\pi/2$ as its argument increases. Thus, introducing the scaling factors in $\bar{\theta}_{jd}$ and $\bar{\phi}_{jd}$ results in $\theta_{jd} \in (-\theta_{\max}, \theta_{\max})$ and $\phi_{jd} \in (-\phi_{\max}, \phi_{\max})$, and the aggressiveness of the UAV's maneuvers can be managed.

Now that the desired orientation has been found, next define the attitude tracking error as

$$e_{j\Theta} = \Theta_{jd} - \Theta_j \in E^a \tag{22}$$

where the dynamics are found using (4) to be $\dot{e}_{j\Theta} = \dot{\Theta}_{jd} - T_j\omega_j$. In order to drive the orientation errors (22) to zero, the desired angular velocity, ω_{jd}, is selected as

$$\omega_{jd} = T_j^{-1}(\dot{\Theta}_{jd} + K_{j\Theta}e_{j\Theta}) \tag{23}$$

where $K_{j\Theta} = diag\{k_{j\Theta 1}, k_{j\Theta 2}, k_{j\Theta 3}\} \in \Re^{3x3}$ is a diagonal positive definite design matrix all with positive design constants. Define the angular velocity tracking error as

$$e_{j\omega} = \omega_{jd} - \omega_j \tag{24}$$

and observing $\omega_j = \omega_{jd} - e_{j\omega}$, the closed loop orientation tracking error system can be written as

$$\dot{e}_{j\Theta} = -K_{j\Theta}e_{j\Theta} + T_je_{j\omega} \tag{25}$$

Examining (23), calculation of the desired angular velocity requires knowledge of $\dot{\Theta}_{jd}$; however, $\dot{\Theta}_{jd}$ is not known in view of the fact $\dot{\Lambda}_j$ and $\dot{\hat{f}}_{jc1}$ are not available. Further, development of u_{j2} in the following section will reveal $\dot{\omega}_{jd}$ is required which in turn implies $\ddot{\Lambda}_j$ and $\ddot{\hat{f}}_{jc1}$ must be known. Since these requirements are not practical, the *universal approximation property* of NN is invoked to estimate ω_{jd} and $\dot{\omega}_{jd}$ (Dierks and Jagannathan, 2008).

To aid in the NN virtual control development, the desired orientation, $\Theta_{jd} \in E^a$, is reconsidered in the fixed body frame, E^b, using the relation $\dot{\Theta}_{jd}^b = T_j^{-1}\dot{\Theta}_{jd}$. Rearranging (23), the dynamics of the proposed virtual controller when the all dynamics are known are revealed to be

$$\dot{\Theta}_{jd}^b = \omega_{jd} - T_j^{-1}K_{j\Theta}e_{j\Theta}$$
$$\dot{\omega}_{jd} = \dot{T}_j^{-1}(\dot{\Theta}_{jd} + K_{j\Theta}e_{j\Theta}) + T_j^{-1}(\ddot{\Theta}_{jd} + K_{j\Theta}\dot{e}_{j\Theta}) \tag{26}$$

For convenience, we define a change of variable as $\Omega_d = \omega_d - T^{-1}K_\Theta e_\Theta$, and the dynamics (26) become

$$\dot{\Theta}_{jd}^b = \Omega_{jd}$$
$$\dot{\Omega}_{jd} = \dot{T}_j^{-1}\dot{\Theta}_{jd} + T_j^{-1}\ddot{\Theta}_{jd} = f_{j\Omega}(x_{j\Omega}) = f_{j\Omega} \tag{27}$$

Defining the estimates of Θ_{jd}^b and Ω_{jd} to be $\hat{\Theta}_{jd}^b$ and $\hat{\Omega}_{jd}$, respectively, and the estimation error $\tilde{\Theta}_{jd}^b = \Theta_{jd}^b - \hat{\Theta}_{jd}^b$, the dynamics of the proposed NN virtual control inputs become

$$\dot{\hat{\Theta}}_{jd}^b = \hat{\Omega}_{jd} + K_{j\Omega1}\tilde{\Theta}_{jd}^b$$

$$\dot{\hat{\Omega}}_{jd} = \hat{f}_{j\Omega} + K_{j\Omega2}\tilde{\Theta}_{jd}^b \qquad (28)$$

where $K_{j\Omega1}$ and $K_{j\Omega2}$ are positive constants. The estimate $\hat{\omega}_{jd}$ is then written as

$$\hat{\omega}_{jd} = \hat{\Omega}_{jd} + K_{j\Omega3}\tilde{\Theta}_{jd}^b + T_j^{-1}K_{j\Theta}e_{j\Theta} \qquad (29)$$

where $K_{j\Omega3}$ is a positive constant.

In (28), *universal approximation property* of NN has been utilized to estimate the unknown function $f_{j\Omega}(x_{j\Omega})$ by bounded ideal weights $W_{j\Omega}^T, V_{j\Omega}^T$ such that $\|W_{j\Omega}\|_F \le W_{M\Omega}$ for a known constant $W_{M\Omega}$, and written as $f_{j\Omega}(x_{j\Omega}) = W_{j\Omega}^T\sigma(V_{j\Omega}^Tx_{j\Omega}) + \varepsilon_{j\Omega}$ where $\varepsilon_{j\Omega}$ is the bounded NN approximation error such that $\|\varepsilon_{j\Omega}\| \le \varepsilon_{\Omega M}$ for a known constant $\varepsilon_{\Omega M}$. The NN estimate of $f_{j\Omega}$ is written as $\hat{f}_{j\Omega} = \hat{W}_{j\Omega}^T\sigma(V_{j\Omega}^T\hat{x}_{j\Omega}) = \hat{W}_{j\Omega}^T\hat{\sigma}_{j\Omega}$ where $\hat{W}_{j\Omega}^T$ is the NN estimate of $W_{j\Omega}^T$ and $\hat{x}_{j\Omega}$ is the NN input written in terms of the virtual control estimates, desired trajectory, and the UAV velocity. The NN input is chosen to take the form of $\hat{x}_\Omega = [1 \ \Lambda_j^T \ \left(\Theta_{jd}^b\right)^T \ \hat{\Omega}_{jd}^T \ v_j^T \ \omega_j^T]^T$.

Observing $\tilde{\omega}_{jd} = \omega_{jd} - \hat{\omega}_{jd} = \tilde{\Omega}_{jd} - K_{j\Omega3}\tilde{\Theta}_{jd}^b$, subtracting (28) from (27) and adding and subtracting $W_{j\Omega}^T\hat{\sigma}_{j\Omega}$, the virtual controller estimation error dynamics are found to be

$$\dot{\tilde{\Theta}}_{jd}^b = \tilde{\omega}_{jd} - (K_{j\Omega1} - K_{j\Omega3})\tilde{\Theta}_{jd}^b$$

$$\dot{\tilde{\Omega}}_{jd} = \tilde{f}_{j\Omega} - K_{j\Omega2}\tilde{\Theta}_{jd}^b + \xi_{j\Omega} \qquad (30)$$

where $\tilde{\Omega}_{jd} = \Omega_{jd} - \hat{\Omega}_{jd}$, $\tilde{f}_{j\Omega} = \tilde{W}_{j\Omega}^T\hat{\sigma}_{j\Omega}$, $\tilde{W}_{j\Omega}^T = W_{j\Omega}^T - \hat{W}_{j\Omega}^T$, $\xi_{j\Omega} = \varepsilon_{j\Omega} + W_{j\Omega}^T\tilde{\sigma}_{j\Omega}$, and $\tilde{\sigma}_{j\Omega} = \sigma_{j\Omega} - \hat{\sigma}_{j\Omega}$. Furthermore, $\|\xi_{j\Omega}\| \le \xi_{\Omega M}$ with $\xi_{\Omega M} = \varepsilon_{\Omega M} + 2W_{M\Omega}\sqrt{N_\Omega}$ a computable constant with N_Ω the constant number of hidden layer neurons in the virtual control NN. Similarly, the estimation error dynamics of (29) are found to be

$$\dot{\tilde{\omega}}_{jd} = -K_{j\Omega3}\tilde{\omega}_{jd} + \tilde{f}_{j\Omega} - \overline{K}_{j\Omega}\tilde{\Theta}_{jd}^b + \xi_{j\Omega} \qquad (31)$$

where $\overline{K}_{j\Omega} = K_{j\Omega2} - K_{j\Omega3}(K_{j\Omega1} - K_{j\Omega3})$. Examination of (30) and (31) reveals $\tilde{\Theta}_{jd}^b$, $\tilde{\omega}_{jd}$, and $\tilde{f}_{j\Omega}$ to be equilibrium points of the estimation error dynamics when $\|\xi_{j\Omega}\| = 0$.

To this point, the desired translational velocity for follower j has been identified to ensure the leader-follower objective (8) is achieved. Then, the desired pitch and roll were derived to drive $v_{jxb} \rightarrow v_{jdx}$ and $v_{jyb} \rightarrow v_{jdy}$, respectively. Then, the desired angular velocity was found to ensure $\Theta_j \rightarrow \Theta_{jd}$. What remains is to identify the UAV thrust to guarantee $v_{jzb} \rightarrow v_{jdz}$ and rotational torque vector to ensure $\omega_j \rightarrow \omega_{jd}$. First, the thrust is derived.

Consider again the translational velocity tracking error dynamics (16), as well as the *desired* velocity tracking error dynamics (18). Equating (16) and (18) and manipulating the third error state, the required thrust is found to be

$$u_{j1} = m_j c_{\bar{\theta}jd} c_{\bar{\phi}jd} (\Lambda_{j3} - g) + m_j (c_{\bar{\phi}jd} s_{\bar{\theta}jd} c_{\psi jd} + s_{\bar{\phi}jd} s_{\psi jd}) \Lambda_{j1}$$
$$+ m_j (c_{\bar{\phi}jd} s_{\bar{\theta}jd} s_{\psi jd} - s_{\bar{\phi}jd} c_{\psi jd}) \Lambda_{j2} + m_j k_{jvz} e_{vj3} + m_j \hat{f}_{jc13} \tag{32}$$

where $\hat{f}_{jc13}$ is the NN estimate in (17) previously defined. Substituting the desired pitch (20), roll (21), and the thrust (32) into the translational velocity tracking error dynamics (16) yields

$$\dot{e}_{jv} = -K_{jv} e_{jv} + A_{jc1} (W_{jc1}^T \sigma_{jc1} + \varepsilon_{jc}) - A_{jc1} \hat{W}_{jc1}^T \hat{\sigma}_{jc1} - K_{j\rho} R_i e_{iv} - \bar{\tau}_{jd1},$$

and adding and subtracting $A_{jc1} W_{jc1}^T \hat{\sigma}_{jc1}^T$ reveals

$$\dot{e}_{jv} = -K_{jv} e_{jv} + A_{jc1} \tilde{W}_{jc1}^T \hat{\sigma}_{jc1} - K_{j\rho} R_i e_{iv} + \xi_{jc1} \tag{33}$$

with $\xi_{jc1} = A_{jc1} W_{jc1}^T \tilde{\sigma}_{jc1}^T + A_{jc1} \varepsilon_{jc1} - \bar{\tau}_{jd1}$, $\tilde{W}_{jc1} = W_{jc1} - \hat{W}_{jc1}$, and $\tilde{\sigma}_{jc1} = \sigma_{jc1} - \hat{\sigma}_{jc1}$. Further, $\|A_{jc1}\|_F = A_{c1\max}$ for a known constant $A_{c1\max}$, and $\|\xi_{jc1}\| \leq \xi_{Mc1}$ for a computable constant $\xi_{Mc1} = A_{c1\max} \varepsilon_{Mc1} + 2 A_{c1\max} W_{Mc1} \sqrt{N_c} + \tau_M / m_j$.

Next, the rotational torque vector, u_{j2}, will be addressed. First, multiply the angular velocity tracking error (24) by the inertial matrix J_j, take the first derivative with respect to time, and substitute the UAV dynamics (1) to reveal

$$J_j \dot{e}_{j\omega} = f_{j2}(x_{jc2}) - u_{j2} - \tau_{jd2} \tag{34}$$

with $f_{jc2}(x_{jc2}) = J_j \dot{\omega}_{jd} - S(J_j \omega_j) \omega_j - N_{j2}(\omega_j)$. Examining $f_{jc2}(x_{jc2})$, it is clear that the function is nonlinear and contains unknown terms; therefore, the *universal approximation property* of NN is utilized to estimate the function $f_{jc2}(x_{jc2})$ by bounded ideal weights W_{jc2}^T, V_{jc2}^T such that $\|W_{jc2}\|_F \leq W_{Mc2}$ for a known constant W_{Mc2} and written as $f_{jc2}(x_{jc2}) = W_{jc2}^T \sigma(V_{jc2}^T x_{jc2}) + \varepsilon_{jc2}$ where ε_{jc2} is the bounded NN functional reconstruction error such that $\|\varepsilon_{jc2}\| \leq \varepsilon_{Mc2}$ for a known constant ε_{Mc2}. The NN estimate of f_{jc2} is given by

$\hat{f}_{jc2} = \hat{W}_{jc2}^T \sigma(V_{jc2}^T \hat{x}_{jc2}) = \hat{W}_{jc2}^T \hat{\sigma}_{jc2}$ where $\hat{W}_{jc2}^T$ is   the   NN   estimate   of W_{jc2}^T and
$\hat{x}_{jc2} = [1 \; \omega_j^T \; \dot{\hat{\Omega}}_{jd}^T \; \widetilde{\Theta}_{jd}^{b\;T} \; e_{j\Theta}^T]^T$ is the input to the NN written in terms of the virtual controller

estimates.   By the construction of the virtual controller, $\dot{\hat{\omega}}_{jd}$ is not directly available;

therefore, observing (29), the terms $\dot{\hat{\Omega}}_{jd}^T$, $\widetilde{\Theta}_{jd}^{b\;T}$, and $e_{j\Theta}^T$ have been included instead.

Using the NN estimate $\hat{f}_{jc2}$ and the estimated desired angular velocity tracking

error $\hat{e}_{j\omega} = \hat{\omega}_{jd} - \omega_j$, the rotational torque control input is written as

$$u_{j2} = \hat{f}_{jc2} + K_{j\omega} \hat{e}_{j\omega}, \tag{35}$$

and substituting the control input (35) into the angular velocity dynamics (34) as well as
adding and subtracting $W_{jc2}^T \hat{\sigma}_{jc}$, the closed loop dynamics become

$$J_j \dot{e}_{j\omega} = -K_{j\omega} e_{j\omega} + \widetilde{W}_{jc2}^T \hat{\sigma}_{jc2} + K_{j\omega} \widetilde{\omega}_{jd} + \xi_{jc2}, \tag{36}$$

where $\widetilde{W}_{jc2}^T = W_{jc2}^T - \hat{W}_{jc2}^T$, $\xi_{jc2} = \varepsilon_{jc2} + W_{jc2}^T \widetilde{\sigma}_{jc} - \tau_{jd2}$, and $\widetilde{\sigma}_{jc2} = \sigma_{jc2} - \hat{\sigma}_{jc2}$. Further, $\|\xi_{jc2}\| \le \xi_{Mc2}$

for a computable constant $\xi_{Mc2} = \varepsilon_{Mc2} + 2W_{Mc2}\sqrt{N_{c2}} + \tau_{dM}$ where N_{c2} is the number of hidden layer

neurons.

As a final step, we define $\widetilde{W}_{jc} = [\widetilde{W}_{jc1} \; 0; \; 0 \; \widetilde{W}_{jc2}]$ and $\hat{\sigma}_{jc} = [\hat{\sigma}_{jc1}^T \; \hat{\sigma}_{jc2}^T]^T$ so that a single

NN can be utilized with N_c hidden layer neurons to represent $\hat{f}_{jc} = [\hat{f}_{jc1}^T \; \hat{f}_{jc2}^T]^T \in \Re^6$. In

the following theorem, the stability of the follower j is shown while considering $e_{iv} = 0$. In
other words, the position, orientation, and velocity tracking errors are considered along
with the estimation errors of the virtual controller and the NN weight estimation errors of
each NN for follower j while ignoring the interconnection errors between the leader and its
followers. This assumption will be relaxed in the following section.

Theorem 3.1.1: (Follower UAV System Stability) Given the dynamic system of follower j in the
form of (1), let the desired translational velocity for follower j to track be defined by (12)
with the desired pitch and roll defined by (20) and (21), respectively. Let the NN virtual
controller be defined by (28) and (29), respectively, with the NN update law given by

$$\dot{\hat{W}}_{j\Omega} = F_{j\Omega} \hat{\sigma}_{j\Omega} \left(\widetilde{\Theta}_{jd}^b\right)^T - \kappa_{j\Omega} F_{j\Omega} \hat{W}_{j\Omega}, \tag{37}$$

where $F_{j\Omega} = F_{j\Omega}^T > 0$ and $\kappa_{j\Omega} > 0$ are design parameters. Let the dynamic NN controller
for follower j be defined by (32) and (35), respectively, with the NN update given by

$$\dot{\hat{W}}_{jc} = F_{jc} \hat{\sigma}_{jc} \left(A_{jc} \hat{e}_{jS}\right)^T - \kappa_{jc} F_{jc} \hat{W}_{jc}, \tag{38}$$

where $A_{jc} = [A_{jc1} \ 0_{3x3}; 0_{3x3} \ I_{3x3}] \in \Re^{6x6}, \hat{e}_{jS} = \left[e_{jv}^T \ \hat{e}_{j\omega}^T\right]^T, F_{jc} = F_{jc}^T > 0$ and $\kappa_{jc} > 0$ are   constant design parameters.   Then there exists positive design constants $K_{j\Omega1}, K_{j\Omega2}, K_{j\Omega3}$, and positive definite design matrices $K_{j\rho}, K_{j\Theta}, K_{jv}, K_{j\omega}$, such that the virtual controller estimation errors $\widetilde{\Theta}_{jd}^b, \widetilde{\omega}_{jd}$ and the virtual control NN weight estimation errors, $\widetilde{W}_{j\Omega}$, the position, orientation, and translational and angular velocity tracking errors, $e_{j\rho}, e_{j\Theta}, e_{jv}, e_{j\omega}$, respectively, and the dynamic controller NN weight estimation errors, $\widetilde{W}_{jc}$, are all *SGUUB*.

Proof: Consider the following positive definite Lyapunov candidate

$$V_j = V_{j\Omega} + V_{jc}, \tag{39}$$

where

$$V_{j\Omega} = \frac{1}{2}\widetilde{\Theta}_{jd}^{b}{}^{T}\overline{K}_{j\Omega}\widetilde{\Theta}_{jd}^{b} + \frac{1}{2}\widetilde{\omega}_{jd}{}^{T}\widetilde{\omega}_{jd} + \frac{1}{2}tr\{\widetilde{W}_{j\Omega}^{T}F_{j\Omega}^{-1}\widetilde{W}_{j\Omega}\}$$

$$V_{jc} = \frac{1}{2}e_{j\rho}^{T}e_{j\rho} + \frac{1}{2}e_{j\Theta}^{T}e_{j\Theta} + \frac{1}{2}e_{jv}^{T}e_{jv} + \frac{1}{2}e_{j\omega}^{T}J_j e_{j\omega} + \frac{1}{2}tr\left\{\widetilde{W}_{jc}^{T}F_{jc}^{-1}\widetilde{W}_{jc}\right\}$$

whose first derivative with respect to time is given by $\dot{V}_j = \dot{V}_{j\Omega} + \dot{V}_{jc}$. Considering first $\dot{V}_{j\Omega}$, and substituting the closed loop virtual control estimation error dynamics (30) and (31) as well as the NN tuning law (37), reveals

$$\dot{V}_{j\Omega} = -\overline{K}_{j\Omega2}\widetilde{\Theta}_{jd}^{b}{}^{T}\widetilde{\Theta}_{jd}^{b} - K_{j\Omega3}\widetilde{\omega}_{jd}{}^{T}\widetilde{\omega}_{jd} + \widetilde{\omega}_{jd}{}^{T}\xi_{j\Omega} + tr\left\{\widetilde{W}_{j\Omega}^{T}\left(\kappa_{j\Omega}\hat{W}_{j\Omega} - \hat{\sigma}_{j\Omega}\left(\widetilde{\Theta}_{jd}^{b}\right)^{T} + \hat{\sigma}_{j\Omega}\widetilde{\omega}_{jd}{}^{T}\right)\right\}$$

where $\overline{K}_{j\Omega2} = (K_{j\Omega1} - K_{j\Omega3})\left(K_{j\Omega2} - K_{j\Omega3}(K_{j\Omega1} - K_{j\Omega3})\right)$ and $\overline{K}_{j\Omega2} > 0$ provided $K_{j\Omega1} > K_{j\Omega3}$ and $K_{j\Omega2} > K_{j\Omega3}(K_{j\Omega1} - K_{j\Omega3})$.   Observing $\|\hat{\sigma}_{j\Omega}\| \le \sqrt{N_{j\Omega}}$, $\|W_{\Omega j}\|_F \le W_{M\Omega}$ for a known constant, $W_{M\Omega}$, and $tr\{\widetilde{W}_{j\Omega}^T(W_{j\Omega} - \widetilde{W}_{j\Omega})\} \le \|\widetilde{W}_{j\Omega}\|_F W_{M\Omega} - \|\widetilde{W}_{j\Omega}\|_F^2$, $\dot{V}_{j\Omega}$ can then be rewritten as

$$\dot{V}_\Omega \le -\overline{K}_{j\Omega2}\left\|\widetilde{\Theta}_{jd}^{b}\right\|^2 - K_{j\Omega3}\left\|\widetilde{\omega}_{jd}\right\|^2 - \kappa_{j\Omega}\left\|\widetilde{W}_{j\Omega}\right\|_F^2 + \left\|\widetilde{\omega}_{jd}\right\|\xi_{\Omega M} + \left\|\widetilde{\Theta}_{jd}^{b}\right\|\left\|\widetilde{W}_{j\Omega}\right\|_F\sqrt{N_{j\Omega}} + \left\|\widetilde{\omega}_{jd}\right\|\left\|\widetilde{W}_{j\Omega}\right\|_F\sqrt{N_{j\Omega}} + \kappa_{j\Omega}\left\|\widetilde{W}_{j\Omega}\right\|_F W_{M\Omega}.$$

Now, completing the squares with respect to $\left\|\widetilde{W}_{j\Omega}\right\|_F, \left\|\widetilde{\Theta}_{jd}^{b}\right\|$, and $\left\|\widetilde{\omega}_{jd}\right\|$, an upper bound for $\dot{V}_{j\Omega}$ is found to be

$$\dot{V}_{j\Omega} \le -\left(\overline{K}_{j\Omega2} - \frac{N_{j\Omega}}{\kappa_{j\Omega}}\right)\left\|\widetilde{\Theta}_{jd}^{b}\right\|^2 - \left(\frac{K_{j\Omega3}}{2} - \frac{N_{j\Omega}}{\kappa_{j\Omega}}\right)\left\|\widetilde{\omega}_{jd}\right\|^2 - \frac{\kappa_{j\Omega}}{4}\left\|\widetilde{W}_{j\Omega}\right\|_F^2 + \eta_{j\Omega} \tag{40}$$

where $\eta_{j\Omega} = \kappa_{j\Omega}W_{M\Omega}^2 + \xi_{\Omega M}^2 / (2K_{j\Omega3})$.   Next, considering $\dot{V}_{jc}$ and substituting the closed loop kinematics (14) and (25), dynamics (33) and (36), and NN tuning law (38) while considering $e_{iv} = 0$ reveals

$$\dot{V}_{jc} = -e_{j\rho}^T K_{j\rho} e_{j\rho} - e_{j\Theta}^T K_{j\Theta} e_{j\Theta} - e_{jv}^T K_{jv} e_{jv} - e_{j\omega}^T K_{j\omega} e_{j\omega} + e_{j\rho}^T R_j e_{jv} + e_{j\Theta}^T T_j e_{j\omega} + e_{jv}^T \xi_{jc1} + e_{j\omega}^T K_{j\omega} \widetilde{\omega}_{jd} + e_{j\omega}^T \xi_{jc2}$$
$$+ \kappa_{jc} tr\left\{ \widetilde{W}_{jc}^T (W_{jc} - \widetilde{W}_{jc}) \right\} + tr\left\{ \widetilde{W}_{jc}^T \hat{\sigma}_{jc2} (e_{j\omega}^T - \hat{e}_{j\omega}^T) \right\}$$

Then, observing $\widetilde{\omega}_{jd} = e_{j\omega} - \hat{e}_{j\omega}$ and completing the squares with respect to $e_{j\rho}, e_{j\Theta}, e_{jv}, e_{j\omega}$ and $\widetilde{W}_{jc}$, and upper bound for $\dot{V}_{jc}$ is found to be

$$\dot{V}_{jc} \le -\frac{K_{j\rho\min}}{2}\|e_{j\rho}\|^2 - \frac{K_{j\Theta\min}}{2}\|e_{j\Theta}\|^2 - \left(\frac{K_{jv\min}}{2} - \frac{R_{\max}^2}{2K_{\rho\min}}\right)\|e_{jv}\|^2 - \frac{\kappa_{jc}}{3}\|\widetilde{W}_{jc}\|_F^2 - \left(\frac{K_{j\omega\min}}{3} - \frac{T_{\max}^2}{2K_{j\Theta\min}}\right)\|e_{j\omega}\|^2 \qquad (41)$$
$$+ \frac{3K_{j\omega\min}}{4}\|\widetilde{\omega}_{jd}\|^2 + \frac{3N_{jc}}{4\kappa_{jc}}\|\widetilde{\omega}_{jd}\|^2 + \eta_{jc}$$

where $K_{j\rho\min}, K_{j\Theta\min}, K_{jv\min}$, and $K_{j\omega\min}$ are the minimum singular values of $K_{j\rho}, K_{j\Theta}, K_{jv}$, and $K_{j\omega}$, respectively, and $\eta_{jc} = \xi_{c1M}^2/(2K_{jv\min}) + \xi_{c2M}^2/(2K_{j\omega\min}) + 3W_{Mc}\kappa_{jc}/4$. Now, combining (40) and (41), an upper bound for $\dot{V}_j$ is written as

$$\dot{V}_j \le -\left(\overline{K}_{j\Omega} - \frac{N_{j\Omega}}{\kappa_{j\Omega}}\right)\|\widetilde{\Theta}_{jd}^b\|^2 - \left(\frac{K_{j\Omega3}}{2} - \frac{N_{j\Omega}}{\kappa_{j\Omega}} - \frac{3K_{j\omega\min}}{4} - \frac{3N_{jc}}{4\kappa_{jc}}\right)\|\widetilde{\omega}_{jd}\|^2 - \frac{K_{j\rho\min}}{2}\|e_{j\rho}\|^2 - \frac{K_{j\Theta\min}}{2}\|e_{j\Theta}\|^2 \qquad (42)$$
$$-\left(\frac{K_{jv\min}}{2} - \frac{R_{\max}^2}{2K_{\rho\min}}\right)\|e_{jv}\|^2 - \left(\frac{K_{j\omega\min}}{3} - \frac{T_{\max}^2}{2K_{j\Theta\min}}\right)\|e_{j\omega}\|^2 - \frac{\kappa_{j\Omega}}{4}\|\widetilde{W}_{j\Omega}\|_F^2 - \frac{\kappa_{jc}}{3}\|\widetilde{W}_{jc}\|_F^2 + \eta_{j\Omega} + \eta_{jc}$$

Finally, (42) is less than zero provided

$$\overline{K}_{j\Omega2} > \frac{N_{j\Omega}}{\kappa_{j\Omega}}, \quad K_{j\Omega3} > \frac{2N_{j\Omega}}{\kappa_{j\Omega}} + \frac{3K_{j\omega\min}}{2} + \frac{3N_{jc}}{2\kappa_{jc}}, \quad K_{jv\min} > \frac{R_{\max}^2}{K_{\rho\min}}, \quad K_{j\omega\min} > \frac{3T_{\max}^2}{2K_{j\Theta\min}} \qquad (43)$$

and the following inequalities hold:

$$\|\widetilde{\Theta}_{jd}^b\| > \sqrt{\frac{\eta_{j\Omega} + \eta_{jc}}{\overline{K}_{j\Omega2} - N_{j\Omega}/\kappa_{j\Omega}}} \quad or \quad \|\widetilde{W}_{jc}\|_F > \sqrt{\frac{3(\eta_{j\Omega} + \eta_{jc})}{\kappa_{jc}}} \quad or \quad \|e_{jv}\| > \sqrt{\frac{2(\eta_{j\Omega} + \eta_{jc})}{K_{jv\min} - R_{\max}^2/K_{\rho\min}}} \qquad (44)$$

$$or \quad \|e_{j\rho}\| > \sqrt{\frac{2(\eta_{j\Omega} + \eta_{jc})}{K_{j\rho\min}}} \quad or \quad \|e_{j\Theta}\| > \sqrt{\frac{2(\eta_{j\Omega} + \eta_{jc})}{K_{j\Theta\min}}} \quad or \quad \|\widetilde{W}_{j\Omega}\|_F > \sqrt{\frac{4(\eta_{j\Omega} + \eta_{jc})}{\kappa_{j\Omega}}}$$

$$or \quad \|e_{j\omega}\| > \sqrt{\frac{\eta_{j\Omega} + \eta_{jc}}{K_{j\omega\min}/3 - T_{\max}^2/(2K_{j\Theta\min})}} \quad or \quad \|\widetilde{\omega}_{jd}\| > \sqrt{\frac{\eta_{j\Omega} + \eta_{jc}}{\frac{K_{j\Omega3}}{2} - \frac{N_{j\Omega}}{\kappa_{j\Omega}} - \frac{3K_{j\omega\min}}{4} - \frac{3N_{jc}}{4\kappa_{jc}}}}$$

Therefore, it can be concluded using standard extensions of Lyapunov theory (Lewis et al., 1999) that $\dot{V}_j$ is less than zero outside of a compact set, revealing the virtual controller estimation errors, $\widetilde{\Theta}_{jd}^b, \widetilde{\omega}_{jd}$, and the NN weight estimation errors, $\widetilde{W}_{j\Omega}$, the position,

orientation, and translational and angular velocity tracking errors, $e_{j\rho}, e_{j\Theta}, e_{jv}, e_{j\omega}$, respectively, and the dynamic controller NN weight estimation errors, $\widetilde{W}_{jc}$, are all *SGUUB*.

3.2 Formation Leader Control Law

The dynamics and kinematics for the formation leader are defined similarly to (1) and (4), respectively. In our previous work (Dierks and Jagannathan, 2008), an output feedback control law for a single quadrotor UAV was designed to ensure the robot tracks a desired path, $\rho_{id} = [x_{id}, y_{id}, z_{id}]^T$, and desired yaw angle, ψ_{id}. Using a similarly approach to (10)-(14), the state feedback control velocity for leader *i* is given by (Dierks and Jagannathan, 2008)

$$v_{id} = [v_{idx} \ v_{idy} \ v_{idz}]^T = R_i^T(\dot{\rho}_{id} + K_{i\rho}e_{i\rho}) \in E^b \quad (45)$$

The closed loop position tracking error then takes the form of

$$\dot{e}_{i\rho} = -K_{i\rho}e_{i\rho} + R_i\,e_{iv} \quad (46)$$

Then, using steps similar to (15)-(21), the desired pitch and roll angles are given by

$$\theta_{id} = \frac{2\theta_{max}}{\pi}a\tan\left(\frac{N_{i\theta d}}{D_{i\theta d}}\right) \quad (47)$$

where $N_{i\theta d} = c_{i\psi d}(\ddot{x}_{id} + k_{i\rho x}\dot{x}_{id} - v_{iR1}) + s_{i\psi d}(\ddot{y}_{id} + k_{i\rho y}\dot{y}_{id} - v_{iR2}) + k_{iv1}e_{vx} + \hat{f}_{ic11}$ and $D_{i\theta d} = \ddot{z}_{id} + k_{i\rho z}\dot{z}_{id} - v_{iR3} - g$ and

$$\phi_{id} = \frac{2\phi_{max}}{\pi}a\tan\left(\frac{N_{i\phi d}}{D_{i\phi d}}\right) \quad (48)$$

where $N_{i\phi d} = s_{i\psi d}(\ddot{x}_{id} + k_{i\rho x}\dot{x}_{id} - v_{iR1}) - c_{i\psi d}(\ddot{y}_{id} + k_{i\rho y}\dot{y}_{id} - v_{iR2}) - k_{iv2}e_{vy} + \hat{f}_{ic12}$, $D_{\phi d} = c_{\bar{\theta}di}(\ddot{z}_{id} + k_{i\rho z}\dot{z}_{id} - v_{iR3} - g) + s_{\bar{\theta}id}c_{\psi id}(\ddot{x}_{id} + k_{i\rho x}\dot{x}_{id} - v_{iR1}) + s_{\bar{\theta}di}s_{\psi id}(\ddot{y}_{id} + k_{i\rho y}\dot{y}_{id} - v_{iR2})$ with $v_{iR} = [v_{iR1} \ v_{iR2} \ v_{iR3}]^T = K_{i\rho}R_iv_i$ and $\hat{f}_{ic1} = [\hat{f}_{ic11} \ \hat{f}_{ic12} \ \hat{f}_{ic13}]^T \in \Re^3$ is a NN estimate of the unknown function $f_{ic1}(x_{ic1})$ (Dierks and Jagannathan, 2008). The desired angular velocity as well as the NN virtual controller for the formation leader is defined similarly to (23) and (28) and (29), respectively, and finally, the thrust and rotation torque vector are found to be

$$u_{i1} = m_i c_{\bar{\theta}id}c_{\bar{\phi}id}(\ddot{z}_{id} + k_{i\rho z}\dot{z}_{id} - v_{iR3} - g) + m_i(c_{\bar{\phi}id}s_{\bar{\theta}id}s_{\psi id} - s_{\bar{\phi}id}c_{\psi id})(\ddot{y}_{id} + k_{i\rho y}\dot{y}_{id} - v_{iR2}) + m_i k_{iv3}e_{ivz}$$
$$+ m_i(c_{\bar{\phi}id}s_{\bar{\theta}id}c_{\psi id} + s_{\bar{\phi}id}s_{\psi id})(\ddot{x}_{id} + k_{i\rho x}\dot{x}_{id} - v_{iR1}) + m_i\hat{f}_{ic13} \quad (49)$$

$$u_{i2} = \hat{f}_{ic2} + K_{i\omega}\hat{e}_{i\omega} \quad (50)$$

where $\hat{f}_{ic2} \in \Re^3$ is a NN estimate of the unknown function $f_{ic2}(x_{ic2})$ and $\hat{e}_{i\omega} = \hat{\omega}_{id} - \omega_i$. The closed loop orientation, virtual control, and velocity tracking error dynamics for the

formation leader are found to take a form similar to (25), (30) and (31), and (33) and (36), respectively (Dierks and Jagannathan, 2008).

Next, the stability of the entire formation is considered in the following theorem while considering the interconnection errors between the leader and its followers.

3.3 Quadrotor UAV Formation Stability

Before proceeding, it is convenient to define the following augmented error systems consisting of the position and translational velocity tracking errors of leader i and N follower UAV's as

$$e_\rho = \left[e_{i\rho}^T \ e_{j\rho}^T \big|_{j=1} \ .... \ e_{j\rho}^T \big|_{j=N} \right]^T \in \Re^{3(N+1)}$$

$$e_v = \left[e_{iv}^T \ e_{jv}^T \big|_{j=1} \ .... \ e_{jv}^T \big|_{j=N} \right]^T \in \Re^{3(N+1)}.$$

Next, the transformation matrix (2) is augmented as

$$R_F = diag\left\{ R_i, R_j \big|_{j=1},..., R_j \big|_{j=N} \right\} \in \Re^{3(N+1)x3(N+1)} \tag{51}$$

while the NN weights for the translational velocity error system are augmented as

$$\hat{W}_{c1} = diag\left\{ \hat{W}_{ic1}, \hat{W}_{jc1} \big|_{j=1},..., \hat{W}_{jc1} \big|_{j=N} \right\} \in \Re^{(N \cdot N_{jc1}+N_{ic1})x3(N+1)}$$

$$\hat{\sigma}_{c1} = \left[\hat{\sigma}_{ic1}^T \ \hat{\sigma}_{jc1}^T \big|_{j=1},..., \hat{\sigma}_{jc1}^T \big|_{j=N} \right]^T \in \Re^{(N \cdot N_{jc1}+N_{ic1})}$$

Now, using the augmented variables above, the augmented closed loop position and translational velocity error dynamics for the entire formation are written as

$$\dot{e}_\rho = -K_\rho e_\rho + (I - G_F)R_F e_v \tag{52}$$

$$\dot{e}_v = -K_v e_v + A_{cF} \tilde{W}_{c1}^T \hat{\sigma}_{c1} - K_\rho G_F R_F e_v + \xi_{c1} \tag{53}$$

where $A_{cF} = diag\left\{ A_{ic}, A_{jc} \big|_{j=1},.., A_{jc} \big|_{j=N} \right\}$ with A_{ic} defined similarly to A_{jc} in terms of $\bar{\Theta}_{id}$, $K_\rho = diag\left\{ K_{i\rho}, K_{j\rho} \big|_{j=1},...K_{j\rho} \big|_{j=N} \right\}$, $K_v = diag\left\{ K_{iv}, K_{jv} \big|_{j=1},...,K_{jv} \big|_{j=N} \right\}$, G_F is a constant matrix relating to the formation interconnection errors defined as

$$G_F = [0 \ 0; F_T \ 0] \in \Re^{(N+1)x(N+1)} \tag{54}$$

and $F_T \in \Re^{NxN}$ is constant and dependent on the specific formation topology. For instance, in a string formation where each follower follows the UAV directly in front of it, follower 1 tracks leader i, follower 2 tracks follower 1, etc., and F_T becomes the identity matrix.

In a similar manner, we define augmented error systems for the virtual controller, orientation, and angular velocity tracking systems as

$$\widetilde{\Theta}_d^b = \left[(\widetilde{\Theta}_{id}^b)^T, (\widetilde{\Theta}_{jd}^b)^T \Big|_{j=1} ... (\widetilde{\Theta}_{jd}^b)^T \Big|_{j=N} \right]^T \in \Re^{3(N+1)}, \ \widetilde{\omega}_d = \left[\widetilde{\omega}_{id}^T, \widetilde{\omega}_{jd}^T \Big|_{j=1} ... \widetilde{\omega}_{jd}^T \Big|_{j=N} \right]^T \in \Re^{3(N+1)},$$

$$e_\Theta = \left[e_{i\Theta}^T \ e_{j\Theta}^T \Big|_{j=1} .... e_{j\Theta}^T \Big|_{j=N} \right]^T \in \Re^{3(N+1)}, \ e_\omega = \left[e_{i\omega}^T \ e_{j\omega}^T \Big|_{j=1} .... e_{j\omega}^T \Big|_{j=N} \right]^T \in \Re^{3(N+1)}, \quad (55)$$

respectively. It is straight forward to verify that the error dynamics of the augmented variables (55) takes the form of (30), (31), (25), and (36), respectively, but written in terms of the augmented variables (55).

Theorem 3.3.1: (UAV Formation Stability) Given the leader-follower criterion of (8) with 1 leader and *N* followers, let the hypotheses of *Theorem 3.1.1* hold. Let the virtual control system for the leader *i* be defined similarly to (28) and (29) with the virtual control NN update law defined similarly to (37). Let control velocity and desire pitch and roll for the leader be given by (45), (47), and (48), respectively, along with the thrust and rotation torque vector defined by (49) and (50), respectively, and let the control NN update law be defined identically to (38). Then, the position, orientation, and velocity tracking errors, the virtual control estimation errors, and the NN weights for each NN for the entire formation are all *SGUUB*.

Proof: Consider the following positive definite Lyapunov candidate

$$V = V_\Omega + V_c, \quad (56)$$

where

$$V_\Omega = \frac{1}{2} \widetilde{\Theta}_d^{b\,T} \overline{K}_\Omega \widetilde{\Theta}_d^b + \frac{1}{2} \widetilde{\omega}_d^T \widetilde{\omega}_d + \frac{1}{2} tr\{ \widetilde{W}_\Omega^T F_\Omega^{-1} \widetilde{W}_\Omega \}$$

$$V_c = \frac{1}{2} e_\rho^T e_\rho + \frac{1}{2} e_\Theta^T e_\Theta + \frac{1}{2} e_v^T e_v + \frac{1}{2} e_\omega^T J e_\omega + \frac{1}{2} tr\{ \widetilde{W}_c^T F_c^{-1} \widetilde{W}_c \}$$

with $\overline{K}_\Omega = diag\{ \overline{K}_{i\Omega} I, \overline{K}_{j\Omega} I \big|_{j=1} ... \overline{K}_{j\Omega} I \big|_{j=N} \}$, $\widetilde{W}_\Omega = diag\{ \widetilde{W}_{i\Omega}, \widetilde{W}_{j\Omega} \big|_{j=1} ... \widetilde{W}_{j\Omega} \big|_{j=N} \}$, $J = diag\{ J_i, J_j \big|_{j=1} ... J_j \big|_{j=N} \}$, and $\widetilde{W}_c = diag\{ \widetilde{W}_{ic}, \widetilde{W}_{jc} \big|_{j=1} ... \widetilde{W}_{jc} \big|_{j=N} \}$. The first derivative of (56) with respect to time is given by $\dot{V} = \dot{V}_\Omega + \dot{V}_c$, and performing similar steps as those used in (40)-(41) reveals

$$\dot{V}_\Omega \le -\left(\overline{K}_{\Omega 2\min} - \frac{N_\Omega}{\kappa_{\Omega\min}} \right) \left\| \widetilde{\Theta}_d^b \right\|^2 - \left(\frac{K_{\Omega 3\min}}{2} - \frac{N_\Omega}{\kappa_{\Omega\min}} \right) \left\| \widetilde{\omega}_d \right\|^2 - \frac{\kappa_\Omega}{4} \left\| \widetilde{W}_\Omega \right\|_F^2 + \eta_\Omega' \quad (57)$$

$$\dot{V}_c \le -\frac{K_{\rho\min}}{2} \left\| e_\rho \right\|^2 - \frac{K_{\Theta\min}}{2} \left\| e_\Theta \right\|^2 - \left(\frac{K_{v\min}}{2} - \frac{\eta_1^2}{2K_{\rho\min}} - \eta_2 \right) \left\| e_{jv} \right\|^2 - \frac{\kappa_{c\min}}{3} \left\| \widetilde{W}_c \right\|_F^2 - \left(\frac{K_{\omega\min}}{3} - \frac{(N+1)T_{\max}^2}{2K_{\Theta\min}} \right) \left\| e_\omega \right\|^2, \quad (58)$$

$$+ \frac{3K_{\omega\min}}{4} \left\| \widetilde{\omega}_d \right\|^2 + \frac{3N_c}{4\kappa_{c\min}} \left\| \widetilde{\omega}_d \right\|^2 + \eta_c$$

where $\overline{K}_{\Omega 2\min}$ is the minimum singular value of $\overline{K}_{2\Omega}$, $\kappa_{\Omega\min}$ is the minimum singular value of $\kappa_{\Omega} = diag\{\kappa_{i\Omega}I, \kappa_{j\Omega}I|_{j=1} ... \kappa_{j\Omega}I|_{j=N}\}$ with I being the identity matrix, $K_{\Omega 3\min}$ is the minimum singular value of $K_{\Omega 3} = diag\{K_{i\Omega 3}I, K_{j\Omega}3I|_{j=1} ... K_{j\Omega 3}I|_{j=N}\}$, N_{Ω} is the number of hidden layer neurons in the augmented virtual control system, and η_{Ω} is a computable constant based on $\eta_{i\Omega}$ and $\eta_{j\Omega}, j = 1, ... N$. Similarly, $K_{\rho\min}, K_{\Theta\min}, K_{v\min}, K_{\omega\min}$, and $\kappa_{c\min}$ are the minimum singular values of the augmented gain matrices $K_{\rho}, K_{\Theta}, K_{v}, K_{\omega}$, and κ_{c} respectively, where $\eta_1 = R_{F\max}\sqrt{1+2N}$, $\eta_2 = K_{\rho\min}R_{F\max}\sqrt{N}$ are a known computable constants and η_c is a computable constant dependent on η_{ic} and $\eta_{jc}, j = 1, ... N$. Now, using (57) and (58), an upper bound for $\dot{V}$ is found to be

$$\dot{V}_{\Omega} \le -\left(\overline{K}_{\Omega 2\min} - \frac{N_{\Omega}}{\kappa_{\Omega\min}}\right)\left\|\widetilde{\Theta}_d^b\right\|^2 - \left(\frac{K_{\Omega 3\min}}{2} - \frac{N_{\Omega}}{\kappa_{\Omega\min}} - \frac{3K_{\omega\min}}{4} - \frac{3N_c}{4\kappa_{c\min}}\right)\left\|\widetilde{\omega}_d\right\|^2 - \frac{\kappa_{\Omega}}{4}\left\|\widetilde{W}_{\Omega}\right\|_F^2 - \frac{\kappa_{c\min}}{3}\left\|\widetilde{W}_c\right\|_F^2 \quad (59)$$
$$- \frac{K_{\rho\min}}{2}\left\|e_{\rho}\right\|^2 - \frac{K_{\Theta\min}}{2}\left\|e_{\Theta}\right\|^2 - \left(\frac{K_{v\min}}{2} - \frac{\eta_1^2}{2K_{\rho\min}} - \eta_2\right)\left\|e_{jv}\right\|^2 - \left(\frac{K_{\omega\min}}{3} - \frac{(N+1)T_{\max}^2}{2K_{\Theta\min}}\right)\left\|e_{\omega}\right\|^2 + \eta_c + \eta_{\Omega}$$

Finally, (59) is less than zero provided

$$\overline{K}_{\Omega 2\min} > \frac{N_{\Omega}}{\kappa_{\Omega\min}}, \quad K_{\Omega 3\min} > \frac{2N_{\Omega}}{\kappa_{\Omega\min}} + \frac{3K_{\omega\min}}{2} + \frac{3N_c}{2\kappa_{c\min}}, \quad K_{v\min} > \frac{\eta_1^2}{K_{\rho\min}} + 2\eta_2, \quad K_{\omega\min} > \frac{3(N+1)T_{\max}^2}{2K_{\Theta\min}} \quad (60)$$

and the following inequalities hold:

$$\left\|\widetilde{\Theta}_d^b\right\| > \sqrt{\frac{\eta_{\Omega} + \eta_c}{\overline{K}_{\Omega 2\min} - N_{\Omega}/\kappa_{\Omega\min}}} \quad or \quad \left\|\widetilde{W}_c\right\|_F > \sqrt{\frac{3(\eta_{\Omega} + \eta_{jc})}{\kappa_{c\min}}} \quad or \quad \left\|e_{jv}\right\| > \sqrt{\frac{2(\eta_{\Omega} + \eta_c)}{K_{v\min} - \eta_1^2/K_{\rho\min} - 2\eta_2}} \quad (61)$$
$$or \quad \left\|e_{\rho}\right\| > \sqrt{\frac{2(\eta_{\Omega} + \eta_c)}{K_{\rho\min}}} \quad or \quad \left\|e_{\Theta}\right\| > \sqrt{\frac{2(\eta_{\Omega} + \eta_c)}{K_{\Theta\min}}} \quad or \quad \left\|\widetilde{W}_{\Omega}\right\|_F > \sqrt{\frac{4(\eta_{\Omega} + \eta_c)}{\kappa_{\Omega\min}}}$$
$$or \quad \left\|e_{\omega}\right\| > \sqrt{\frac{\eta_{\Omega} + \eta_c}{K_{\omega\min}/3 - (N+1)T_{\max}^2/(2K_{\Theta\min})}} \quad or \quad \left\|\widetilde{\omega}_d\right\| > \sqrt{\frac{\eta_{\Omega} + \eta_c}{\frac{K_{\Omega 3\min}}{2} - \frac{N_{\Omega}}{\kappa_{\Omega\min}} - \frac{3K_{\omega\min}}{4} - \frac{3N_c}{4\kappa_{c\min}}}}$$

Therefore, it can be concluded using standard extensions of Lyapunov theory (Lewis et al., 1999) that $\dot{V}$ is less than zero outside of a compact set, revealing the position, orientation, and velocity tracking errors, the virtual control estimation errors, and the NN weights for each NN for the entire formation are all *SGUUB*.

Remark 3: The conclusions of *Theorem 3.3.1* are independent of any specific formation topology, and the Lyapunov candidate (56) represents the most general form required show the stability of the entire formation. Examining (60) and (61), the minimum controller gains and error bounds are observed to increase with the number of follower UAV's, *N*. These results are not surprising since increasing number of UAV's increases the sources of errors which can be propagated throughout the formation.

Remark 4: Once a specific formation as been decided and the form of F_T is set, the results of *Theorem 3.3.1* can be reformulated more precisely. For this case, the stability of the formation is proven using the sum of the individual Lyapunov candidates of each UAV as opposed to using the augmented error systems (51)-(55).

4. Optimized energy-delay sub-network routing (OEDSR) protocol for UAV Localization and Discovery

In the previous section, a group of UAV's was modeled as a nonlinear interconnected system. We have shown that the basic formation is stable and each follower achieves its separation, angle of incidence, and bearing relative to its leader with a bounded error. The controller assignments for the UAV's can be represented as a graph where a directed edge from the leader to the followers denotes a controller for the followers while the leader is trying to track a desired trajectory. The shape vector consists of separations and orientations which in turn determines the relative positions of the follower UAV's with respect to its leader.

Then, a group of N UAV's is built on two networks: a physical network that captures the constraints on the dynamics of the lead UAV and a sensing and communication network, preferably wireless, that describes information flow, sensing and computational aspects across the group. The design of the graph is based on the task in hand. In this graph, nodes and edges represent UAV's and control policies, respectively. Any such graph can be described by its adjacency matrix (Das et al., 2002).

In order to solve the leader-follower criterion (8), ad hoc networks are formed between the leader(s) and the follower(s), and the position of each UAV in the formation must be determined on-line. This network is dependent upon the sensing and communication aspects. As a first step, a leader is elected similar to the case of multi-robot formations (Das et al., 2002) followed by the discovery process in which the sensory information and physical networks are used to establish a wireless network. The outcome of the leader election process must be communicated to the followers in order to construct an appropriate shape. To complete the leader-follower formation control task (8), the controllers developed in the previous section require only a single-hop protocol; however, a multi-hop architecture is useful to relay information throughout the entire formation like the outcome of the leader election process, changing tasks, changing formations, as well alerting the UAV's of approaching moving obstacles that appear in a sudden manner.

The optimal energy-delay sub-network routing (OEDSR) protocol (Jagannathan, 2007) allows the UAV's to communicate information throughout the formation wirelessly using a multi-hop manner where each UAV in the formation is treated as a hop. The energy-delay routing protocol can guarantee information transfer while minimizing energy and delay for real-time control purposes even for mobile ad hoc networks such as the case of UAV formation flying.

We envision four steps to establish the wireless ad hoc network. As mentioned earlier, leader election process is the first step. The discovery process is used as the second step where sensory information and the physical network are used to establish a spanning tree. Since this is a multi-hop routing protocol, the communication network is created on-demand unlike in the literature where a spanning tree is utilized. This on-demand nature would allow the UAV's to be silent when they are not being used in communication and

generate a communication path when required. The silent aspect will reduce any inference to others. Once a formation becomes stable, then a tree can be constructed until the shape changes. The third step will be assignment of the controllers online to each UAV based on the location of the UAV. Using the wireless network, localization is used to combine local sensory information along with information obtained via routing from other UAV's in order to calculate relative positions and orientations. Alternatively, range sensors provide relative separations, angles of incidence, and bearings. Finally cooperative control allows the graph obtained from the network to be refined. Using this graph theoretic formulation, a group is modeled by a tuple $\Gamma = (\vartheta, \mathrm{P}, \mathrm{H})$ where ϑ is the reference trajectory of the robot, P represents the shape vectors describing the relative positions of each vehicle with respect to the formation reference frame (leader), and H is the control policy represented as a graph where nodes represent UAV and edges represent the control assignments. Next, we describe the OEDSR routing protocol where each UAV will be referred to as a "node."

In OEDSR, sub-networks are formed around a group of nodes due to an activity, and nodes wake up in the sub-networks while the nodes elsewhere in the network are in sleep mode. An appropriate percentage of nodes in the sub-network are elected as cluster heads (CHs) based on a metric composed of available energy and relative location to an event (Jagannathan, 2007) in each sub-network. Once the CHs are identified and the nodes are clustered relative to the distance from the CHs, the routing towards the formation leader (FL) is initiated. First, the CH checks if the FL is within the communication range. In such case, the data is sent directly to the FL. Otherwise, the data from the CHs in the sub-network are sent over a multi-hop route to the FL. The proposed routing algorithm is fully distributed since it requires only local information for constructing routes, and is proactive adapting to changes in the network. The FL is assumed to have sufficient power supply, allowing a high power beacon from the FL to be sent such that all the nodes in the network have knowledge of the distance to the FL. It is assumed that all UAV's in the network can calculate or measure the relative distance to the FL at any time instant using the formation graph information or local sensory data. Though the OEDSR protocol borrows the idea of an energy-delay metric from OEDR (Jagannathan, 2007), selection of relay nodes (RN) does not maximize the number of two hop neighbors. Here, any UAV can be selected as a RN, and the selection of a relay node is set to maximize the link cost factor which includes distance from the FL to the RN.

4.1 Selection of an Optimum Relay-Node-Based link cost factor

Knowing the distance information at each node will allow the UAV to calculate the Link Cost Factor (LCF). The link cost factor from a given node to the next hop node 'k' is given by (62) where D_k represent the delay that will be incurred to reach the next hop node in range, the distance between the next hop node to the FL is denoted by Δx_k, and the remaining energy, E_k, at the next hop node are used in calculation of the link cost as

$$LCF_k = \frac{E_k}{D_k \cdot \Delta x_k} \qquad (62)$$

In equation (62), checking the remaining energy at the next hop node increases network lifetime; the distance to the FL from the next hop node reduces the number of hops and end-to-end delay; and the delay incurred to reach the next hop node minimizes any channel problems. When multiple RNs are available for routing of the information, the optimal RN is selected based on the highest LCF. These clearly show that the proposed OEDSR protocol is an on demand routing protocol. For detailed discussion of OEDSR refer to (Jagannathan, 2007). The route selection process is illustrated through the following example. This represents sensor data collected by a follower UAV for the task at hand that is to be transmitted to the FL.

4.2 Routing Algorithm through an Example
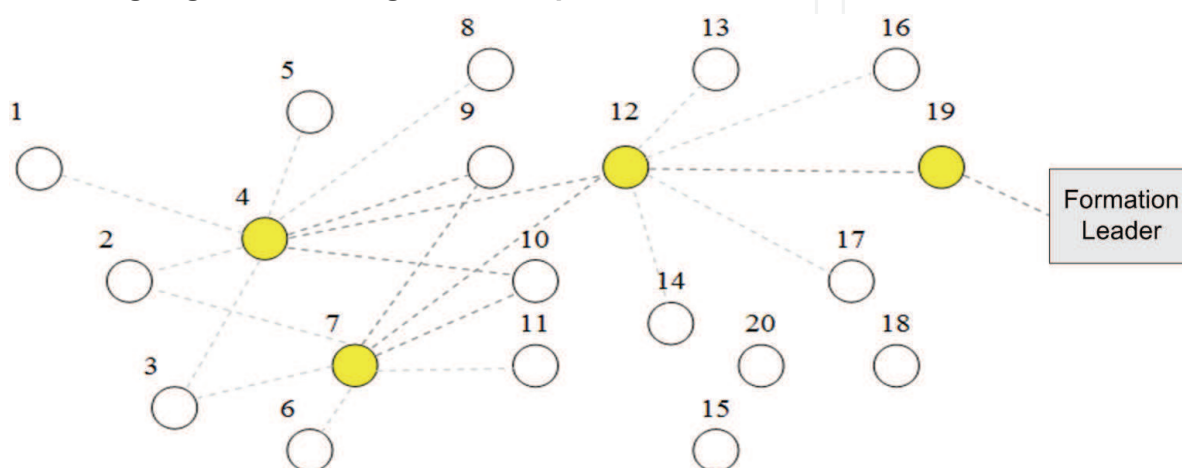
Figure 2. Relay node selection

Consider the formation topology shown in Figure 2. The link cost factors are taken into consideration to route data to the FL. The following steps are implemented to route data using the OEDSR protocol:

1. Start with an empty relay list for source UAV n: $Relay(n)=\{ \}$. Here UAV n_4 and n_7 are CHs.
2. First, CH n_4 checks with which nodes it is in range with. In this case, CH n_4 is in range with nodes n_1, n_2, n_3, n_5, n_8, n_9, n_{12}, and n_{10}.
3. The nodes n_1, n_2, and n_3 are eliminated as potential RNs because the distance from them to the FL is greater than the distance from CH n_4 to the FL.
4. Now, all the nodes that are in range with CH n_4 transmit RESPONSE packets and CH n_4 makes a list of possible RNs, which in this case are n_5, n_8, n_9, n_{12}, and n_{10}.
5. CH n_4 sends this list to CH n_7. CH n_7 checks if it is range with any of the nodes in the list.
6. Nodes n_9, n_{10}, and n_{12} are the nodes that are in range with both CH n_4 and n_7. They are selected as the potential common RNs.
7. The link cost factors for n_9, n_{10}, and n_{12} are calculated.
8. The node with the maximum value of LCF is selected as the RN and assigned to *Relay(n)*. In this case, *Relay(n)={n12}*.
9. Now UAV n_{12} checks if it is in direct range with the FL, and if it is, then it directly routes the information to the FL.

10. Otherwise, n_{12} is assigned as the RN, and all the nodes that are in range with node n_{12} and whose distance to the FL is less than its distance to the FL are taken into consideration. Therefore, UAV's n_{13}, n_{16}, n_{19}, and n_{17} are taken into consideration.

11. The LCF is calculated for n_{13}, n_{16}, n_{19}, n_{14}, and n_{17}. The node with the maximum LCF is selected as the next RN. In this case $Relay(n) = \{n19\}$.

12. Next the RN n_{19} checks if it is in range with the FL. If it is, then it directly routes the information to the FL. In this case, n_{19} is in direct range, so the information is sent to the FL directly.

4.3 Optimality Analysis for OEDSR

To prove that the proposed route created by OEDSR protocol is optimal in all cases, it is essential to show it analytically.

Assumption 1: It is assumed that all UAV's in the network can calculate or measure the relative distance to the FL at any time instant using the formation graph information or local sensory data.

Theorem 4.3.1: The link cost factor-based routing generates viable RNs to the FL.

Proof: Consider the following two cases

Case I: When the CHs are one hop away from the FL, the CH selects the FL directly. In this case, there is only one path from the CH to the FL. Hence, OEDSR algorithm does not need to be used.

Case II: When the CHs have more than one node to relay information, the OEDSR algorithm selection criteria are taken into account. In Figure 3, there are two CHs, CH_1 and CH_2. Each CH sends signals to all the other nodes in the network that are in range. Here, *CH1* first sends out signals to *n1, n3, n4, and n5* and makes a list of information about the potential RN. The list is then forwarded to *CH2*. *CH2* checks if it is in range with any of the nodes in the list. Here, *n4* and *n5* are selected as potential common RNs. A single node must be selected from both *n4* and *n5* based on the OEDSR link cost factor. The cost to reach *n* from *CH* is given by (2). So based on the OEDSR link cost factor, *n4* is selected as the RN for the first hop. Next, *n4* sends signals to all the nodes it has in range, and selects a node as RN using the link cost factor. The same procedure is carried on till the data is sent to the FL.

Lemma 4.3.2: The intermediate UAV's on the optimal path are selected as RNs by the previous nodes on the path.

Proof: A UAV is selected as a RN only if it has the highest link cost factor and is in range with the previous node on the path. Since OEDSR maximizes the link cost factor, intermediate nodes that satisfy the metric on the optimal path are selected as RNs.

Lemma 4.3.3: A UAV can correctly compute the optimal path (with lower end to end delay and maximum available energy) for the entire network topology.

Proof: When selecting the candidate RNs to the CHs, it is ensured that the distance form the candidate RN to the FL is less than the distance from the CH to the FL. When calculating the link cost factor, available energy is divided by distance and average end-to-end delay to ensure that the selected nodes are in range with the CHs and close to the FL. This helps minimize the number of multi-point RNs in the network.

Theorem 4.3.4: OEDSR protocol results in an optimal route (the path with the maximum energy, minimum average end-to-end delay and minimum distance from the FL) between the CHs and any source destination.
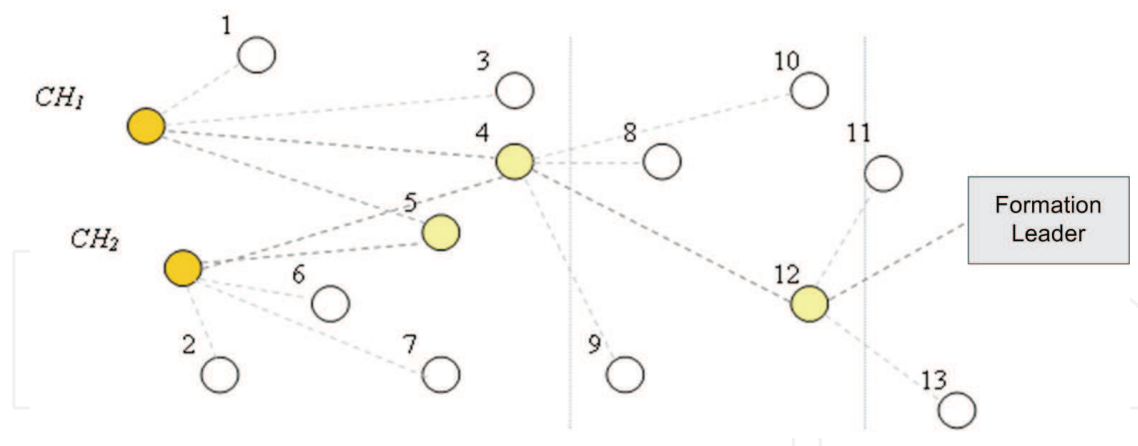
Figure 3. Link cost calculation

5. Simulation Results

A wedge formation of three identical quadrotor UAV's is now considered in MATLAB with the formation leader located at the apex of the wedge. In the simulation, follower 1 should track the leader at a desired separation $s_{jid} = 2\ m$, desired angle of incidence $\alpha_{jid} = 0\ (rad)$, and desired bearing $\beta_{jid} = \pi/3\ (rad)$ while follower 2 tracks the leader at a desired separation $s_{jid} = 2\ m$ desired angle of incidence, $\alpha_{jid} = -\pi/10\ (rad)$, and desired bearing $\beta_{jid} = -\pi/3\ (rad)$. The desired yaw angle for the leader and thus the formation is selected to be $\psi_d = \sin(0.3\pi t)$. The inertial parameters of the UAV's are taken to be as $m = 0.9\ kg$ and $J = diag\{0.32, 0.42, 0.63\}\ kg\ m^2$, and aerodynamic friction is modeled as in (Dierks and Jagannathan, 2008). The parameters outlined in Section 3.3 are communicated from the leader to its followers using single hop communication whereas results for OEDSR in a mobile environment can be found in (Jagannathan, 2007).

Each NN employs 5 hidden layer neurons, and for the leader and each follower, the control gains are selected to be, $K_{\Omega 1} = 23,\ K_{\Omega 2} = 80,\ K_{\Omega 3} = 20,\ K_\rho = diag\{10, 10, 30\}$, $k_{v1} = 10, k_{v2} = 10, k_{v3} = 30,\ K_\Theta = diag\{30, 30, 30\}$, and $K_\omega = diag\{25, 25, 25\}$. The NN parameters are selected as, $F_\Omega = 10, \kappa_\Omega = 1$, and $F_c = 10, \kappa_c = 0.1$, and the maximum desired pitch and roll values are both selected as $2\pi/5$.

Figure 4 displays the quadrotor UAV formation trajectories while Figures 5-7 show the kinematic and dynamic tracking errors for the leader and its followers. Examining the trajectories in Figure 4, it is important to recall that the bearing angle, β_{ji}, is measured in the inertial reference frame of the follower rotated about its yaw angle. Examining the tracking errors for the leader and its followers in Figures 5-7, it is clear that all states track their desired values with small bounded errors as the results of *Theorem 3.3.1* suggest. Initially, errors are observed in each state for each UAV, but these errors quickly vanish as the virtual control NN and the NN in the actual control law learns the nonlinear UAV dynamics. Additionally, the tracking performance of the underactuated states v_x and v_y implies that the desired pitch and roll, respectively, as well as the desired angular velocities generated by the virtual control system are satisfactory.
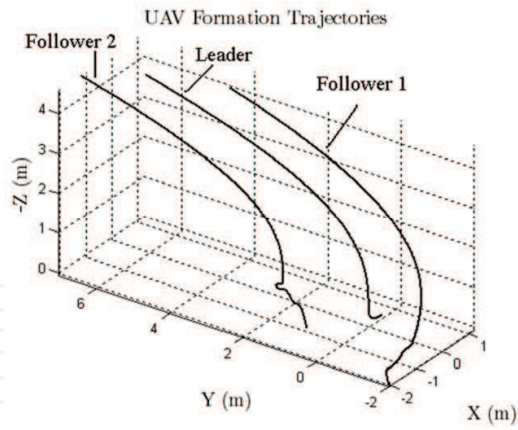
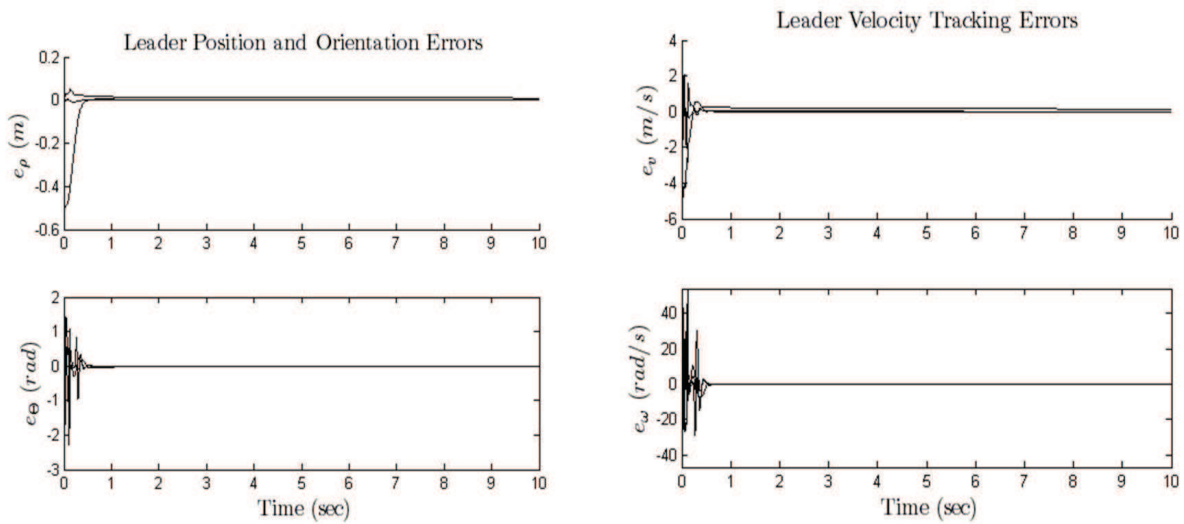Figure 4. Quadrotor UAV formation trajectories

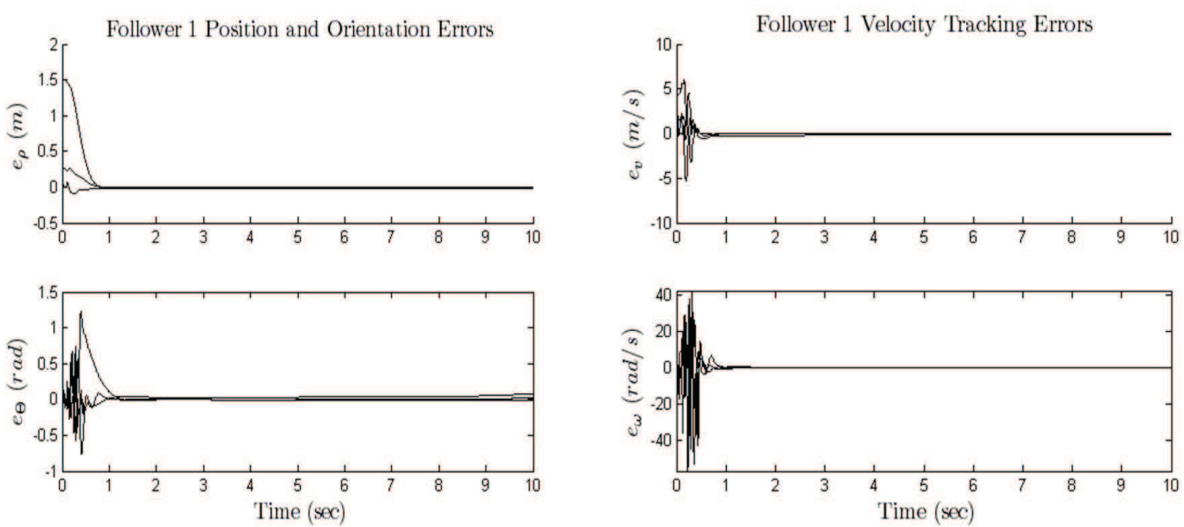Figure 5. Tracking errors for the formation leader
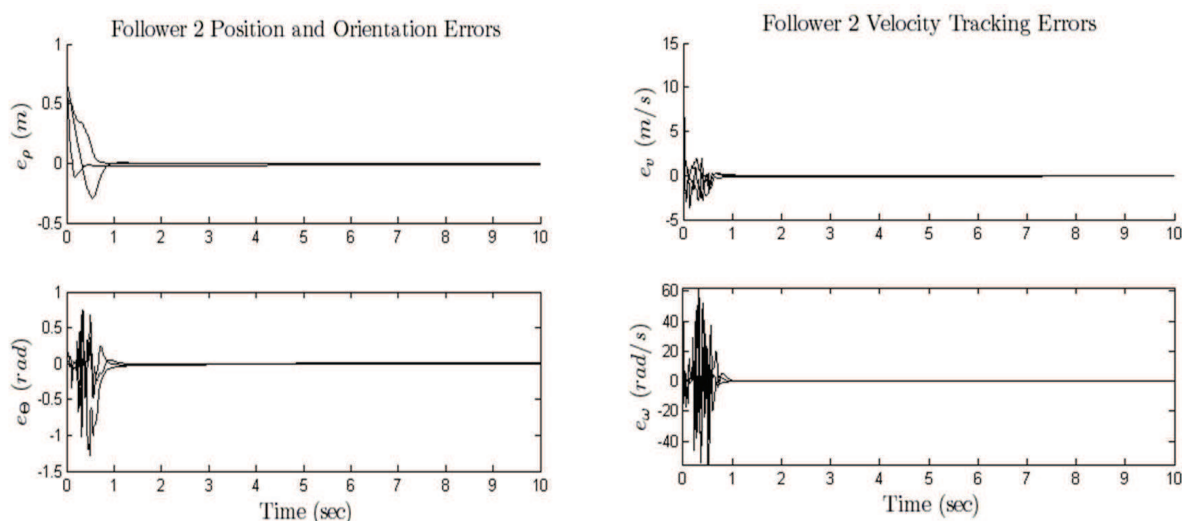

Figure 6. Tracking errors for follower 1

Figure 7. Tracking errors for follower 2

6. Conclusions

A new framework for quadrotor UAV leader-follower formation control was presented along with a novel NN formation control law which allows each follower to track its leader without the knowledge of dynamics. All six DOF are successfully tracked using only four control inputs while in the presence of unmodeled dynamics and bounded disturbances. Additionally, a discovery and localization scheme based on graph theory and ad hoc networks was presented which guarantees optimal use of the UAV's communication links. Lyapunov analysis guarantees *SGUUB* of the entire formation, and numerical results confirm the theoretical conjectures.

7. References

Das, A.; Spletzer, J.; Kumar, V.; & Taylor, C. (2002). Ad hoc networks for localization and control of mobile robots, *Proceedings of IEEE Conference on Decision and Control,* pp. 2978-2983, Philadelphia, PA, December 2002

Desai, J.; Ostrowski, J. P.; & Kumar, V. (1998). Controlling formations of multiple mobile robots, *Proceedings of IEEE International Conference on Robotics and Automation*, pp. 2964-2869, Leuven, Belgium, May 1998

Dierks, T. & Jagannathan, S. (2008). Neural network output feedback control of a quadrotor UAV, *Proceedings of IEEE Conference on Decision and Control*, To Appear, Cancun Mexico, December 2008

Fierro, R.; Belta, C.; Desai, J.; & Kumar, V. (2001). On controlling aircraft formations, *Proceedings of IEEE Conference on Decision and Control*, pp. 1065-1079, Orlando, Florida, December 2001

Galzi, D. & Shtessel, Y. (2006). UAV formations control using high order sliding modes, *Proceedings of IEEE American Control Conference,* pp. 4249-4254, Minneapolis, Minnesota, June 2006

Gu, Y.; Seanor, B.; Campa, G.; Napolitano M.; Rowe, L.; Gururajan, S.; & Wan, S. (2006). Design and flight testing evaluation of formation control laws. *IEEE Transactions on Control Systems Technology*, Vol. 14, No. 6, (November 2006) page numbers (1105-1112)

Jagannathan, S. (2007). *Wireless Ad Hoc and Sensor Networks*, Taylor & Francis, ISBN 0-8247-2675-8, Boca Raton, FL

Lewis, F.L.; Jagannathan, S.; & Yesilderek, A. (1999). *Neural Network Control of Robot Manipulators and Nonlinear Systems*, Taylor & Francis, ISBN 0-7484-0596-8, Philadelphia, PA

Neff, A.E.; DongBin, L.; Chitrakaran, V.K.; Dawson, D.M.; & Burg, T.C. (2007). Velocity control for a quad-rotor uav fly-by-camera interface, *Proceedings of the IEEE Southeastern Conference,* pp. 273-278, Richmond, VA, March 2007

Saffarian, M. & Fahimi, F. (2008). Control of helicopters' formation using non-iterative nonlinear model predictive approach, *Proceedings of IEEE American Control Conference*, pp. 3707-3712, Seattle, Washington, June 2008

Xie, F.; Zhang, X.; Fierro, R; & Motter, M. (2005). Autopilot based nonlinear UAV formation controller with extremum-seeking, *Proceedings of IEEE Conference on Decision and Control*, pp 4933-4938, Seville, Spain, December 2005
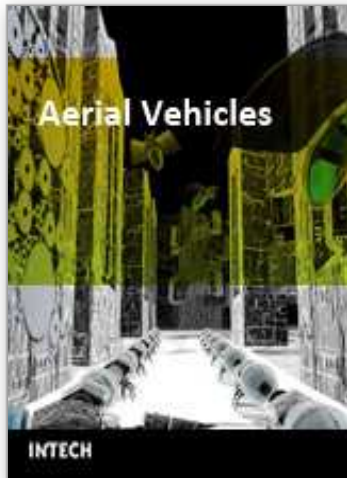
Aerial Vehicles

Edited by Thanh Mung Lam

ISBN 978-953-7619-41-1

Hard cover, 320 pages

Publisher InTech

Published online 01, January, 2009

Published in print edition January, 2009

This book contains 35 chapters written by experts in developing techniques for making aerial vehicles more intelligent, more reliable, more flexible in use, and safer in operation.It will also serve as an inspiration for further improvement of the design and application of aeral vehicles. The advanced techniques and research described here may also be applicable to other high-tech areas such as robotics, avionics, vetronics, and space.

How to reference

In order to correctly reference this scholarly work, feel free to copy and paste the following:

Travis Dierks and S. Jagannathan (2009). Neural Network Control and Wireless Sensor Network-based Localization of Quadrotor UAV Formations, Aerial Vehicles, Thanh Mung Lam (Ed.), ISBN: 978-953-7619-41-1, InTech, Available from:
http://www.intechopen.com/books/aerial_vehicles/neural_network_control_and_wireless_sensor_network-based_localization_of_quadrotor_uav_formations

INTECH
open science | open minds